



# A regional atmosphere-ocean climate system model (CCLMv5.0clm7-NEMOv3.3-NEMOv3.6) over Europe including three marginal seas: on its stability and performance

Cristina Primo<sup>1</sup>, Fanni D. Kelemen<sup>1</sup>, Hendrik Feldmann<sup>2</sup>, Bodo Ahrens<sup>1</sup>

5 <sup>1</sup>Institute for Atmospheric and Environmental Sciences, Goethe University, Frankfurt am Main, Germany,  
<sup>2</sup>Institute of Meteorology and Climate Research, Karlsruhe Institute of Technology, Karlsruhe, Germany,

*Correspondence to:* Cristina Primo (primoram@iau.uni-frankfurt.de)

**Abstract.** The frequency of extreme events has changed, having a direct impact on human lives. Regional climate models help us to predict these regional climate changes. This work presents an atmosphere-ocean coupled regional climate system model (RCSM, with the atmospheric component COSMO-CLM, and the ocean component NEMO) over the European domain, including three marginal seas: the Mediterranean, the North and the Baltic Seas. To test the model, we evaluate a simulation of more than one hundred years (1900-2009) with a spatial grid resolution of about 25km. The simulation was nested into a coupled global simulation with the model MPI-ESM in a low-resolution configuration, whose ocean temperature and salinity were nudged to an MPI-ESM-LR ocean-ice component forced with the 20<sup>th</sup> Century Reanalysis (20CR). The evaluation shows the robustness of the RCSM and discusses the added value by the coupled marginal seas over an atmosphere-only simulation. The coupled system runs stable for the complete 20<sup>th</sup> century and provides a better representation of extreme temperatures compared to the atmosphere-only model. The produced long-term dataset will allow an improved study of extreme events, helping us to better understand the processes leading to meteorological and climate extremes and their prediction.

## 1 Introduction

20 Regional climate affects directly human lives and the socio-economic conditions. The natural variability of the climate system impacts local weather. Due to the recent changes in the frequency and intensity of local extreme events (Tebaldi et al., 2006; Hartmann et al., 2013; Casanueva et al., 2014), like storms or heavy rainfall, we aim at a better understanding of the climate system dynamics. The main components of the Earth climate system are the atmosphere, land, ocean and rivers. To have a better representation of the interactions between the atmosphere and the rest of components of the Earth climate system, it would be necessary to couple models representing all components. However, this is highly complex since it requires combining different numerical models, what may not only bring instabilities, but it also implies high computational costs, etc.. Therefore, current coupled climate systems focus only on a reduced number of these components. Since the oceans are the main boundary of the atmosphere (they cover 71% of the Earth's surface) and their critical role regulating energy flows (they have an enormous heat storage and transport capacity), coupled ocean-atmosphere models have been developed to better understand the



interactions between ocean and atmosphere. For example, the Working Group on Coupled Modelling (WGCM) established the Coupled Model Intercomparison Project (CMIP) as a standard experimental protocol for studying the output of coupled atmosphere-ocean general circulation models (AOGCMs) [<https://cmip.llnl.gov/index.html>]. However, the coarse-resolution of these models does not resolve some physical processes that take place in local scales and that are relevant to understand extreme events like warming and precipitation trends changes. For example, marginal seas are not well represented in general circulation models (Somot et al., 2008; Li et al., 2006). In addition, it has also been proved that the Sea Surface Temperature (SST) has a large spread when comparing an ensemble of AOGCMs (Dommenget, 2012) and that GCM simulations tend to underestimate the high precipitation intensities (Sun et al., 2006). On the other hand, there are very high-resolution process-oriented models, like those used to forecast fog or winter storms (e.g. The Weather Research and Forecasting model, WRF, High Resolution Limited Area Models, HIRLAM, or the High-Resolution Window Forecast System, HIRSW) that resolve those physical processes, but the computational cost is unaffordable to run a long simulation. Therefore, Regional climate systems models (RCSMs) present as an appropriate tool to improve the spatial scale compared to global models, but keeping an affordable computational cost compared to high-resolution process-oriented models.

Within the European region, different atmosphere-ocean-ice coupled RCSMs have been already run for shorter periods (a few decades). For example, Schrum et al. (2003) coupled the regional model REMO (Jacob and Podzun, 1997) and the ocean model HAMSOM (Schrum, 1997) to analyse the North and Baltic Seas, showing the improvements compared to running the uncoupled HAMSOM version. Pham et al. (2014) coupled the regional model COSMO-CLM (Rockel et al., 2008) to the ocean model NEMO (Madec, 2011) for the Baltic and North Seas to evaluate the impact of these seas on the climate of Europe. Sevault et al. (2014) describe and evaluate a fully coupled regional climate system model (CNRM-RCSM4) dedicated to study the Mediterranean climate variability over the period 1980 to 2012, showing a good agreement between the model and observations (e.g seasonal cycle and the interannual variability of SST, sea level, water budget, etc.). In recent studies, Obermann et al. (2018) coupled CCLM with the NEMO setup for the Mediterranean (NEMO-MED12) over the Med-CORDEX domain with ERA-Interim as the driving data. They showed that the coupled system was mostly able to simulate Mistral and Tramontane events with smaller biases than ERA-Interim. Akhtar et al. (2017) used that system to show the impact of the horizontal grid resolution and the dynamic ocean coupling of the NEMO-MED in simulations with the COSMO-CLM during the period from 1979 to 2009 and Hordoier et al. (2018) coupled the NEMO-NORDIC model to CCLM and showed that the high biases presented when compared to observations were of the same magnitude as other COSMO-CLM studies and smaller than for the uncoupled version. Their study covered the period 1979-2007 and they argued that the quality of the model was a result of using ERA-Interim as driving data, whose quality is already high. Nevertheless, all these studies focus only on a few decades, but extreme events have long return periods, so long term simulations are more appropriate to better represent and analyse them. So far, no long-term simulation of more than one hundred years with a regional climate coupled system is available yet. Hence, one of the goals of this work is to fill this gap.

Our aim is to improve our understanding about the regional climate change in Europe and which is the added value by coupling three marginal seas (the Mediterranean, the North and the Baltic Seas). Therefore, this work presents an atmosphere-ocean



RCSM over Europe with a spatial grid resolution of about 25km, and tests its stability and performance with a simulation of more than one hundred years. The added value of the coupling is analysed by comparing our simulation with a centennial atmosphere-only model run. A description about the extra costs due to the coupling compared to an atmosphere-only system is also included. We have particular interest in better understanding changes on extreme events, like heat/cold waves and extreme precipitation, therefore, special focus is placed to analyse the performance of the system representing extremes compared to the atmosphere-only model.

The paper is structured as follows: Section 2 presents the regional climate system models used in this work, namely an atmosphere-only model and an atmosphere-ocean coupled system. Section 3 presents the methods and reference data used to show the stability and performance of the coupled system. Section 4 presents the results of the evaluation of the systems, distinguishing the impact of the coupling over the ocean and the European land. Special attention is given to describe the evolution of climate change indices during the last century. Finally, Section 5 includes a summary with the main conclusions of the study.

## 2 Regional climate system models

This work presents an atmosphere-ocean coupled RCSM and compare it with an atmosphere-only version. This section describes the details about the different components of the RCSM: the atmospheric model, the ocean model, their set-up (lateral and boundary conditions) and how the coupling in the atmosphere-ocean system is done.

### 2.1 Atmospheric model

The three-dimensional non-hydrostatic limited-area atmospheric prediction model COSMO of the German Weather Service has a climate version, the COSMO-CLM (CCLM; Rockel et al., 2008). This is a land-atmosphere regional climate model based on primitive equations that accounts a variety of physical processes by parametrization schemes. The atmospheric model version used in this study is the CCLM v5.0 ctm7 with a numerical time step of 150 seconds and with a third order Runge-Kutta numerical integration scheme. The atmospheric lateral and top boundary condition are given by the atmospheric component of the earth system model of the Max-Planck Institute (MPI-ESM, version 6.1, Stevens et al., 2013). This model couples the atmosphere, ocean and land surface through the exchange of energy, momentum, water and important trace gases such as carbon dioxide. The atmospheric lateral and top boundary conditions of our RCSM, come from a two-step simulation: First an ocean only simulation was performed where the 20<sup>th</sup> Century Reanalysis (20CR, Compo et al., 2011) forced the ocean-ice component of the MPI-ESM, called MPIOM (Müller et al., 2015). From these runs, Müller et al. (2014) took ocean temperature and salinity and nudged them into the coupled global model Max Planck Institute Earth System model in a low-resolution configuration, MPI-ESM-LR (no nudging of atmospheric variables), with the latest version of the ocean model MPIOM (Jungclaus et al., 2013) and the atmospheric component ECHAM6 (Stevens et al., 2013). They run three members, and we considered the first one (as20ncep08\_r1i1p1-LR).



This work compares the atmosphere-only CCLM model with an atmosphere-ocean RCSM. In the coupled version, the prescribed SST of the CCLM over the regional oceans, as well as the fraction of sea ice in the Baltic and North Seas, are replaced by the SST and sea ice fraction given by ocean models presented in the following section, whereas the ocean models receive information from the atmospheric model about the Evaporation-Precipitation, winds and solar fluxes. The MPI-ESM-  
5 LR simulation drives both, the atmosphere-only and the atmosphere-ocean RCSMs. Hence, the SST of the atmosphere-only system is prescribed with the nudged MPI-ESM SST, whereas the SST of the atmosphere-ocean system comes from the ocean model presented below.

Within the Coordinated Regional Downscaling Experiment (CORDEX), a choice of different domains covering the land around the world were defined. Our study aims to better understand the regional climate of central Europe, therefore, the model  
10 runs within the so-called EURO-CORDEX domain (<http://www.cordex.org/domains/cordex-region-euro-cordex/>, see Figure 1 for a representation), with a spatial resolution  $0.22^\circ \times 0.22^\circ$  ( $\sim 25\text{km}$ ,  $226 \times 232 = 52432$  grid points) and 40 vertical levels.

## 2.2 Ocean model

The Nucleus for European Modelling of the Ocean (NEMO) is a flexible tool for studying the interactions of the ocean with the atmosphere over a wide range of space and time scales. Within NEMO, the ocean is interfaced with a sea-ice model (LIM  
15 or CICE), passive tracer and biogeochemical models (TOP) and has the possibility to couple with several atmospheric general circulation models, such as CCLM. High-resolution configurations for the regional oceans in the European domain are available for the NEMO community ocean model. For example, Beuvier et al. (2012) developed MED12, a regional version of the NEMO ocean engine on the Mediterranean Sea. In this work we use NEMO-MED12, based on NEMO version 3.6, with a resolution  $1/12^\circ$  ( $\sim 0.083^\circ \sim 9\text{km}$ ,  $264 \times 567 = 149688$  grid points), 75 vertical levels and with a numerical time step equal to  
20 720 s. The initial conditions for three-dimensional potential temperature and salinity were provided by the MEDATLAS-II (Rixen, 2012) monthly mean seasonal climatology (1945-2002) in the Mediterranean Sea. The Black Sea and runoff water input were prescribed from the climatological average of interannual data from Ludwig et al. (2009). Another NEMO set-up has been adapted to reproduce the barotropic and baroclinic dynamics, as well as the thermohaline structure, of the Baltic and North Sea basins. This is the so-called NEMO-NORDIC (Hordoir et al., 2018), whose ocean component is coupled to the sea  
25 ice model LIM3 (Vancoppenolle et al., 2009). In this study we use NEMO-NORDIC, based on NEMO version 3.3, including the LIM3 sea ice model, with a resolution  $2^\circ$  ( $\sim 0.03^\circ \sim 3\text{km}$ ,  $523 \times 619 = 323737$  grid points), 56 vertical levels and a numerical time step equal to 180 s. The initial conditions for three-dimensional potential temperature and salinity are provided by Janssen et al. (1999) and the lateral boundary conditions in the North Sea are prescribed from ORAS4 reanalysis data (Balmaseda et al., 2013). Freshwater inflow of the rivers is provided from daily time series of the E-HYPE model output (Lindström et al.,  
30 2010). Figure 1 represents the domains where the NEMO-MED and NEMO-NORDIC models run (grey areas).



## 2.2 Coupling

In the atmosphere-ocean climate system, the atmospheric model CCLM is coupled with two configurations of NEMO: one adapted to the Mediterranean Sea (NEMO-MED12) and one to the Baltic/North Seas (NEMO-NORDIC). The coupling is done through a fully parallel communication between parallel models executed via the Model Coupling Toolkit library (MCT; Jacob et al., (2005), named the OASIS3 Model Coupling Toolkit (OASIS3-MCT; Craig et al., 2017), since this library has already been successfully used to couple the CCLM model with NEMO (Will et al., 2017). This is an interface included in CCLM based on the Message Passing Interface (MPI). Including this library significantly improves the performance over the previous version OASIS3, because the bottleneck due to the sequential separate coupler is entirely removed as shown in Gasper et al. (2014). During the coupling, the original ocean domain, which must be smaller than the CCLM domain, is interpolated to the CCLM grid. At runtime, all CCLM ocean grid points located inside the interpolated area are filled with values interpolated from the ocean model and all CCLM ocean grid points located outside the interpolated area are filled with external forcing data.

In addition, OASIS3-MCT offers a performance analysis tool, the LUCIA tool (Maisonave and Caubel, 2014), that measures how much time each system component is spending doing its own calculation (send and receive operations as well as time needed for interpolation of fields) and how much time it is waiting for information coming from the other components. This allows an optimization of the computing time and resources, as well as a comparison with the atmosphere-only system, and the scaling of each model of the coupled system. We have used the LUCIA tool to find an optimal distribution of the available number of cores used for the computation, having in mind that the model with the highest number of grid points of our system is the NEMO-BALTIC. Figure 2 shows an example of a configuration using 11 nodes of MISTRAL, the High-Performance Computing system for Earth system research (HLRE3) at the German High-Performance Computing Centre for Climate and Earth System Research, Germany. We assigned three nodes to CCLM, seven to NEMO-BALTIC and one to NEMO-MED. Like this, only NEMO-MED has to wait for the exchange of the other models, while the other two models require similar times for the calculations. In this configuration, we require around 3.6 times more of the resources used by the non-coupled system (3 nodes for CCLM, compared to 11 for the coupled system). Fig. 2 refers to the time used to send/receive operations and interpolation. To have a complete picture about the costs due to the coupling, we have also done a comparison between the time spent to run one day with the same resources (same number of nodes), using the coupled system compared to the atmosphere-only system (saving the same list of CCLM variables in both versions). For this example, the coupled version takes around five minutes using the 11 nodes, whereas the non-coupled version takes around two minutes if it runs in 3 nodes (i.e. the same number of used nodes by CCLM in the coupled version), and around one minute if we assign all the 11 nodes to run CCLM. So, the coupled system is 5 times slower given the same number of available nodes.



### 3 Methods and reference data

Our aim is to prove that the coupled system runs stable over the whole century and that including the hydrosphere component represented by the Mediterranean Sea and the North and Baltic Seas improves not only the global MPI-ESM-LM simulations, but at least perform as good as the atmosphere-only model.

#### 5 3.1 Methods

To evaluate the stability of the coupled atmosphere-ocean RCM, we have done a spatio-temporal analysis of a centennial simulation (1900-2009). The analysis consists of a study of the temporal series evolution, annual cycles, spatio-temporal density distributions and spatial patterns of three variables of interest: sea surface temperature, the 2m- temperature and the total precipitation. Results were compared to the same analysis obtained with an atmosphere-only (CCLM) version simulation over the same period, run within the national research project on climate prediction MiKlip (“Mittelfristige Klimaprognosen”, Marotzke et al., (2016). The temporal series analysis helped us to detect if the atmosphere-ocean model has any bias or drift compared to the atmosphere-only simulation. The spatial analysis helped us to detect if the system behaves differently according to the area of interest, or if it shows any spatial bias.

Regarding the quality of the coupled model, we compared our simulation with different reference datasets (see next section for more details). Rather than a point-by-point comparison with the reference data, we would like to know if the system represents well the reference’s value distributions, in particular of the extremes. For this purpose, we compared the density distributions and box-plots of our system with those obtained from observational datasets. We analysed the marginal seas separately, distinguishing also among seasons. Regarding the land, different relevant areas have been used in the literature for regional climate studies over Europe, e.g. within the European project PRUDENCE (Prediction of Regional scenarios and Uncertainties for Defining European Climate change Risks and Effects; Christensen, 2005) eight regions were defined: British Isles, Iberian Peninsula, France, Mid-Europe, Scandinavia, Alps, Mediterranean and Eastern Europe. Since we aim to improve our understanding of the regional climate in Germany, we showed some results on the Mid-Europe sub-area.

We are also interested in high-impact phenomena: heavy precipitation, dry spells and heat waves. The joint CCI/CLIVAR/JCOMM Expert Team (ET) on Climate Change Detection and Indices (ETCCDI) suggested a list of 27 core climate change indices based on daily temperature values and daily precipitation amounts (Karl et al., 1999; Zhang et al., 2011). The definition of these indices can be found on the webpage of the project ([etccdi.pacificclimate.org/list\\_27\\_indices.shtml](http://etccdi.pacificclimate.org/list_27_indices.shtml)). We computed these indices, using the free available R package RClimDex, developed and maintained by Xuebin Zhang and Yang Feng at Climate Research Division of the Environment and Climate Change Canada, that in addition to the computation of the indices, also provides simple quality control on the input daily data. We also analysed how the distribution of these indices is represented compared to the distribution of the indices obtained with the observed dataset.



### 3.2 Reference data

To analyse the performance of the system, two centennial reference datasets are available: gridded observations and station observations. Regarding the gridded data, the University of East Anglia produced the gridded Climatic Research Unit (CRU) Time-series (TS) for the period January 1901 – December 2016 (Harris et al., 2014), which consists of monthly data at high-resolution (0.5x0.5 degree) grids. In this work, version 4.01 data (University of East Anglia CRU, 2017) is used. Our simulation has a higher resolution (0.22°x0.22°), therefore it is penalized when comparing to CRU data due to the upscaling. However, there is no available higher resolution gridded dataset covering the complete century. If we want to compare model data with gridded observations with similar spatial resolution, we would have to consider shorter periods. For example, the EOBS data set (Haylock et al., 2008) is available for the last half of the century (from 1950 onwards). E-OBS is a European daily high-resolution gridded data set covering only land between 25N-75N x 40W-75E, obtained from daily observations of precipitation, minimum, maximum and mean surface temperature for the period since 1950. The gridded data is available on different spatial resolutions, in particular on 0.22 degrees rotated grid, like the resolution of the regional climate model used in this work, but it covers only half of our period of interest. Therefore, the downscaled re-analysis produced in this work, helps also to cover the lack of observations during the first half of the century. It is worthy to remark that none of these observational data-sets are perfect, and that they also differ from each other. For example, Fig. 3 shows a comparison of the monthly mean in January 1995, when a flood event happened over Germany. The figure illustrates the information loss regarding the event through upscaling compared to the 0.22° resolution. This fact can penalize our system when comparing it with CRU, especially for the first half of the century, in which EOBS data are not available. Nevertheless, this will not affect the direct comparison of the coupled and atmosphere-only version. To compare our coupled data with centennial observations with higher quality, we can consider historical daily station observations. The Climate Data Center (CDC) of the German Weather Service “Deutscher Wetterdienst” (DWD) provides free access to quality-controlled measurements and observations (climate-stations), derived from DWD stations and legally and qualitatively equivalent partner stations operated for climatological and climate related application (DWD-CDC, 2017). We also quality controlled the data by choosing those stations with less than 15% of missing values and took the stations that covered the complete period (1900-2009), obtaining nine stations distributed over Germany. We chose two of these stations, where no data gap happened during the period, and located at two different altitudes and distances to the seas: Potsdam (circle in Fig.1, located at 81m) and Hohenpeißenberg (triangle at Fig.1, located at 977m). For the sake of brevity, this work presents a comparison of the RCSMs only for the two stations, but similar conclusions were reached by analysing the other seven stations.

With respect to observations over the ocean, unfortunately, there is no high resolution observed data set for the complete period. Hence, we used the Hadley Centre sea ice and sea surface temperature data set (HadISST; Rayner et al. 2003) developed by the Met Office Hadley Centre for Climate Prediction and Research with a 1° resolution to verify our coupled system over the ocean. In addition, we compared the sea surface temperature over the Mediterranean with the NOAA Optimum Interpolation Sea Surface Temperature V2 (OISSTv2; Reynolds et al., 2002) for the available decades (1981-2009). We used



these data even though it only covers a few decades, because the sea surface temperature of the CCLM atmosphere-only simulation is not independent from the HadISST observations (they were used to obtain the MPI-ESM-LR driving simulation). Besides the observations, we also compared the coupled system over the marginal seas with a multi-model ensemble consisting of the first member ('r1i1p1') of eight models from the CMIP5 simulations.

## 5 4 Evaluation results

We based our analyses on three variables: The sea surface temperature, the 2m- temperature and the total precipitation. The behaviour over ocean and land is presented separately. We name the atmosphere-only model (CCLM) uncoupled and the atmosphere-ocean model (CCLM-NEMO) coupled.

### 4.1 Sea surface temperature

10 We analysed the temporal evolution of the SST over the marginal seas (Mediterranean and Baltic/North Seas) to see if there is any drift or evolving bias in the coupled system over the ocean (Figure 4). The long-term SST time series of our coupled system shows a stable system, although the annual mean SST values are colder than the observations (HadISST) and also compared to the uncoupled system in both basins. The SST of the uncoupled system comes from the global system MPI-ESM-LM, whose simulation is not independent from the HadISST observations. Thus, an independent SST observation, namely the  
15 NOAA Optimum Interpolation Sea Surface Temperature V2, is also included for the Mediterranean as a comparison for the available last three decades (1981-2009). Despite of the cold bias, the regional coupled system follows the time evolution of the observed and also the global SST values. In the Mediterranean, it even matches the ensemble mean of the CMIP5 global simulations, and in the Baltic, it is within the spread of this ensemble. Therefore, the SST values from the coupled system have at least as good quality as the values of an average global model, with the advantage of having higher resolution, which  
20 preferably improves the model results especially in the land/sea transition zone.

Figure 5 shows a good representation of the annual cycle for both basins. Dots represent the averaged SST over the whole century per month, and intervals show the 10<sup>th</sup> and 90<sup>th</sup> percentiles. The coupled system is colder than the observations during the whole year, not just in annual average shown in previous figure. In the Mediterranean, the coupled system is colder in the winter and warmer in the summer than the global simulation. In the Baltic and North Sea basin, the coupled system is colder  
25 than the uncoupled and the observations throughout the year.

The density histograms of the three marginal seas summarize both the spatial and the temporal distribution of the SST values (Figure 6). Since the Baltic and North Sea have different climatology in winter due to the presence of ice (the Baltic Sea is colder than the North Sea), we have analysed their histograms separately. In the Mediterranean Sea, the distribution of model data and observations have similar shape, namely a double maximum representing summer and winter temperatures.  
30 Comparing the modelled and the observed histograms, both the coupled and uncoupled models capture the main aspects of the SST distribution. The regional coupled simulation has a wider distribution than the observations, which is made up by a well-





fitting upper range and a shift towards cooler temperatures at the lower range. In comparison with the uncoupled version, the coupled system represents better the upper extremes but has a colder bias on the lower tail. The distribution shape of the uncoupled dataset is very similar to the observation, what might partly be due to that these observations were assimilated indirectly into the simulation of the global model, and the uncoupled version gets them directly from the global model.

5 Nevertheless, the uncoupled model also has a cold bias.

The SST of the coupled version in the Baltic and North Seas comes from the ocean NEMO-NORDIC model, that includes the sea ice and the freezing/melting processes via a sea ice model. This leads to an improvement in the lower tail of the distribution over the Baltic, compared to the uncoupled system that provides much colder temperatures. Both systems have a cold bias on the upper tail. Regarding the North Sea, the coupled model shows a colder bias compared to the uncoupled model.

10 The spatial distribution of the regional coupled system's SST bias shows that the modelled seas, as previously seen, are cooler in all seasons (Figure 7, spring and autumn are not shown). Nevertheless, during winter the basin of the Baltic Sea has a warm bias and during summer the Mediterranean Sea has a gradient in the bias field from south to north.

#### 4.2 2m-Temperature

This section analyses how the coupled system propagates the information received from the ocean about the sea surface  
15 temperature to higher levels, in particular the impact on 2m-temperatures. Figure 8 shows the differences of the 2m-temperature monthly mean, in degrees, between the coupled and uncoupled systems averaged during winter (a) and summer (b) for the period 1901-2009. The plots show differences up to 2.35°C. The coupled system gives colder temperatures over the Mediterranean Sea during the winter, and warmer temperatures during the summer, with the exception of the French coast and north-east coast. Regarding the Baltic and North Seas, the behaviour is not that different in summer and winter. The coupled  
20 model provides colder temperatures over the North Sea and west part of the Baltic Sea, whereas warmer temperatures over the north and eastern part of the Baltic Sea. The boxplots (c) represent the distribution over the marginal seas separately, Baltic/North and Mediterranean Seas, as well as over the land, for each season, over the whole period. A horizontal line is plot as reference of no differences between the systems. The plot shows how the spread of the differences on the Baltic is similar during the year, and the coupled system is mainly colder. The highest spread of the differences happens in the Mediterranean  
25 in summer, where the coupled version is warmer. In winter the spread is smaller and the coupled system is colder. Regarding the land, in summer the boxplot is centred in the zero and with very small spread, showing mainly no difference between the systems. However, there are some outliers where the coupled system shows higher temperatures (with up to 2°C difference). In winter the differences are slightly more noticeable, and the main outliers are negative values, showing that the coupled simulation allows for colder temperatures.

30 Figure 9 shows the temporal evolution of the 2m-temperature annual mean, averaged over the marginal seas. Black lines represent the coupled system and grey lines, the uncoupled. Dashed lines represent a linear fit. The figure shows how both systems represent a similar growing trend, being the coupled system mostly colder than the uncoupled.



### 4.3. Total precipitation

Figure 10 represents the total precipitation monthly sum differences between the coupled and uncoupled system averaged during winter (a) and summer (b). The highest differences happen in winter over the Mediterranean Sea, where the uncoupled system provides more precipitation than the coupled, especially in the eastern part. In summer, however, the coupled system gives more precipitation in this region. Regarding the North Sea, the uncoupled simulation gives in general more precipitation than the coupled. The differences in the Baltic are smaller, being slightly more appreciable in summer than in winter. The differences of the amount of precipitation over the seas are in concordance with the differences of 2m-temperature: the higher 2m-temperature, the more precipitation. Boxplots (c) show the distributions over the marginal seas and land separately. The spread in the Baltic/North is higher in winter, with more outliers, whereas in the Mediterranean is in summer, with more negative outliers (higher precipitation for the uncoupled system). The differences over land are smaller in general, although in winter the outliers are as big as in the Mediterranean. This fact corresponds to the high differences that happen in winter in the Mediterranean coast, where the coupled system is drier, and in the Alpine region, where the coupled system is wetter.

### 4.4 Model-Observations comparison

This section studies the performance of the coupled system in Europe. For this purpose, we compared the model data (coupled and uncoupled systems) with the observed CRU dataset. Data coming from coupled and uncoupled systems were interpolated to the  $0.5^\circ \times 0.5^\circ$  CRU-grid, and only those grid points defined in all three data-sets were considered. Errors of the 2m-temperature of the coupled and uncoupled systems when compared to the CRU observations for winter and summer, the 2m-temperature distributions and the distributions of the 2m-temperature errors are shown in Figure 11. In winter, there is not clear positive or negative bias (Fig11a-b). However, in summer the coupled and uncoupled systems are colder than the CRU observations, apart from the Alpine region and the south-east area, where both systems are warmer (Fig11c-d). Boxplots show a good representation of the observed distribution (Fig11e). In winter distributions are similar and the main differences appear in summer, where the systems show slightly smaller values in the low temperature range. The differences also show similar distribution for coupled and uncoupled systems (Fig11f). As mentioned in Sec. 4.2, the 2m-temperature differences between coupled and not-coupled systems are below  $2.5^\circ\text{C}$ , however boxplots show that the differences compared to CRU are much higher, up to  $10^\circ\text{C}$  in winter. In summer more than 75% of the 2m-temperature given by the systems is colder than the observations. In winter there is no clear bias, and boxplots are centred around the zero value. Nevertheless, there are more extreme higher values (longer upper tail in winter showing higher temperatures for the systems compared to the observations). To compare the annual cycle of both systems with the CRU data, figure 12 represents boxplots corresponding to the annual cycle of the monthly 2m-temperature averaged over the PRUDENCE region namely Mid-Europe for the 20<sup>th</sup> century (a) and the distributions of the differences of the model values minus the CRU observations (b). Both systems show similar distributions than the CRU data in winter, however colder distributions in summer. The differences are centred around the zero value in winter and below zero in summer, that is, on average the winter is better represented by the regional systems than the



summer. However, the spread is much bigger in winter than in summer, that is, in those cases in which the regional systems differ from the CRU observed data, the differences are higher in winter than in summer.

We have also analysed the spatio-temporal distribution to see if the behaviour is different from the averages. Figure 13 shows the density histograms of the 2m-temperature of the coupled and uncoupled systems compared to the CRU data over Mid-  
5 Europe. Blue bars represent the uncoupled system, red bars the coupled system, and white bars the CRU observations. Both systems show a good fit in winter and a colder bias in summer.

### 4.3 Extreme cases

CRU data are monthly values, therefore, cannot be used to analyse extreme events like heat/cold waves or dry/Wet spells. Instead, observed station data provided by the German Weather Service (DWD-CDC, 2017) are considered in this study. We  
10 computed some of the suggested 27 core climate change indices suggested by the ETCCDI over the 20<sup>th</sup> century for the coupled and uncoupled systems, as well as for two long term series of stations located in Germany: Potsdam and Hohenpeißenberg. Figure 14 shows the temporal evolution of four climate change indices: TNn is the annual minimum value of daily minimum temperature, TXx is the annual maximum value of daily maximum temperature, TX90p gives information about the warm  
15 spells since it is defined as the percentage of days when the maximum temperature is above the calendar day 90<sup>th</sup> percentile centred on a 5-day window for the base period 1961-1990. To compute the 90<sup>th</sup> percentile for each calendar day, a bootstrap procedure was used to avoid possible inhomogeneity across the in-base and out-base periods (see details in Zhang et al., 2005). Finally, TN10p gives information about the cold spells since it is defined as the percentage of days when the minimum temperature is below the calendar day 10<sup>th</sup> percentile centred on a 5-day window for the base period 1961-1990. As with  
20 TX90P, the bootstrap procedure is also applied here. Linear trends are shown as dashed lines. Fig. 14 shows how the coupled version also presents a stable evolution of the indices, capturing the trends and improving the uncoupled version for the TNn and TXx indices, especially for the higher station. The coupled system detects the increase of temperature during the century, as well as the increase of the percentage of days with maximum temperatures above the 90<sup>th</sup> percentile, and percentage of days with minimum temperature below the 10<sup>th</sup> percentile.

Figure 15 shows a comparison of the distribution of these indices for the coupled and uncoupled systems and the observations,  
25 based on the quantiles (q-q plot). The diagonal is plot as reference since it represents the perfect case, assuming that observations are perfect. The closer to the diagonal, the better the representation of the observed distribution of the indices. The panels show how the coupled version corrects the overestimation of minimum temperatures of the uncoupled system, as well as the underestimation of the maximum temperatures. Therefore, the coupling has a positive impact with respect to extreme temperatures. Regarding the percentage of days above the 90<sup>th</sup> percentile and below the 10<sup>th</sup> percentile, the coupled  
30 version fits the observed distribution similarly to the uncoupled version, but corrects the extreme cases. In the case of the precipitation, we focus on the following indices (Fig. 16): PRCPTOT is the annual total precipitation in wet days, R95p is the annual total PRCP when the daily precipitation (RR) is above the 95<sup>th</sup> percentile of precipitation on wet days in the 1961-1990 period, CDD is the maximum length of dry spell (maximum number of consecutive days with RR < 1mm) and CWD is the



maximum length of wet spell (maximum number of consecutive days with  $RR \geq 1\text{mm}$ ). In this case, coupled and uncoupled systems also show differences, being the uncoupled system more skilful. The coupled version seems to overestimate the precipitation in Potsdam, but to underestimate it in Hohenpeißenberg. Nevertheless, the coupled system also captures the observed dynamic of the climate change indices related to precipitation. Figure 17 represents the quantile-quantile plot of the coupled (red lines) and uncoupled (blue lines) systems compared to the DWD data for the previous extreme indices of both stations, Potsdam and Hohenpeißenberg. Plots show how lines corresponding to the uncoupled system are closer to the diagonal, representing in a better way the observed quantiles of the extreme precipitation indices. Note that the model data were not bias corrected.

## 5. Summary and Conclusions

To better understand how the Earth climate system evolves in local scales, it is necessary to gain a better understanding of the interactions among the different components of the system. This work presents an atmosphere-ocean coupled regional climate system model (RCSM) over Europe including three marginal seas: The Mediterranean, the Baltic and the North Seas. The coupled system was tested by evaluating a centennial simulation (1900-2009) over the EURO-CORDEX domain on a  $0.22^\circ \times 0.22^\circ$  grid (around 25km). The atmospheric component was given by the COSMO model in the climate mode (COSMO-CLM) and the lower boundary conditions over the sea surfaces by coupling the climate model to two NEMO ocean model setups, the Mediterranean Sea (NEMO-MED12) and the Baltic and North Seas (NEMO-NORDIC). The coupling was made through the OASIS3-MCT coupler. For the lateral and top boundary conditions, the regional atmosphere was forced by the global Earth System Model MPI-ESM, whose ocean was nudged to an MPI-ESM ocean-ice component forced with the 20<sup>th</sup> Century Reanalysis (20CR).

Our aim was to know if the atmosphere-ocean coupled RCSM runs stable within one hundred years and which the cost and benefits of coupling the marginal seas are, specially representing extreme events. We first analysed the computing costs (in terms of resources and time consumed) due to the coupling, showing that 3.6 times more of the resources are required to run the same period or that the coupled version is 5 times slower using the same amount of resources compared to an atmosphere-only version (only the CCLM component). To test the stability of the system during the 20<sup>th</sup> century, we did an analysis on three variables: sea surface temperature (SST), 2m-temperature and total precipitation. Results show that the system runs stable over the whole century, with no drift nor evolving bias. Finally, we evaluated the performance of the coupled RCSM compared to a centennial simulation of the atmosphere-only version, as well as to observations (CRU data and DWD-station observations). We cannot conclude that one system is better than the other, but results depend on the variable, area and season of interest, as explained below.

This study includes a spatio-temporal analysis of the sea surface temperature (SST) of the coupled system (provided by the NEMO ocean-model) over the Mediterranean, North and Baltic Seas, as well as a comparison with the SST of the atmosphere-only version (prescribed with the MPI-ESM-LR SST) and SST observations (HadISST and in case of the Mediterranean Sea also OISSTv2). Results show a stable and realistic evolution of the SST over the century, with a colder bias compared to



observations, but performing similar to the ensemble mean of a global atmosphere-ocean coupled ensemble system. This means that the coupled system provides SSTs on a higher resolution with the added value of preserving the spatial and temporal dynamics (the ensemble mean is not a realization of the system, but an average). The SST annual cycle is well represented. In winter, the coupled system shows a colder bias compared to the uncoupled system in most of the Mediterranean Sea and in the North Sea, whereas a warmer bias in the Baltic Sea and the western part of the Mediterranean. In summer, it shows mostly a colder bias in the three marginal seas, excepting the south-half of the Mediterranean, that shows a positive bias.

Regarding the 2-m temperature, the coupled RCSM increases the 2m-temperature over the Mediterranean Sea in summer and decreases it in winter compared to the atmosphere-only version. It also decreases the 2m-temperature over the North Sea for both seasons, whereas it increases it over the Baltic Sea. Over land differences are smaller on average, but the extreme differences are as high as those found over the sea. Coupled and atmosphere-only systems show a negative bias in summer months compared to the 2m-temperature of the CRU data, whereas a better representation over the winter. However, even though in general the errors are smaller in winter, the extreme error cases also occur in winter. Hence, the spread of the difference distribution is higher in winter than in summer. A comparison of the 2m-temperature annual cycle and the spatio-temporal density distributions within the 20<sup>th</sup> century over the PRUDENCE area namely Mid-Europe is included to show that this behaviour occurs during the whole period.

Regarding the total precipitation, the same pattern as the 2m-temperature is shown: the higher the 2m-temperature, the more precipitation given by the systems. Thus, the coupled system provides less precipitation in the Mediterranean Sea than the uncoupled system during winter, and more during summer. In the Baltic and North seas, the coupled gives in general more precipitation than the uncoupled during both seasons. Over the land, the differences are smaller than over the sea, apart from those happening in the Mediterranean coast in winter, where the coupled system is drier compared to the uncoupled, and in the Alpine region, where the coupled system is wetter compared to the uncoupled.

Special focus was given to the analysis of extreme events. Since this study requires higher temporal precision than the monthly values provided by the CRU data, observations coming from DWD-stations with hourly resolution were considered. The evolution of some climate change indices is presented and discussed, showing that the coupled system is stable and improves the values of the climate change indices related to extreme temperatures compared to the uncoupled version. However, the uncoupled represents in a better way the climate change indices related to precipitation.

To conclude, the centennial atmosphere-ocean coupled simulation presented in this work provides valuable information about the local climate in Europe. Having such a long temporal series of a stable atmosphere-ocean coupled system, whose spatial resolution is higher than the global models, helps us to improve our knowledge of the local phenomena, especially for extreme events that have longer return periods. It has been proved that coupling the ocean improves the representation of heat and cold waves. Our centennial run can also be used to investigate the interactions among different variables on a regional scale and to know more about the atmospheric drivers that lead to extreme events. In addition, these downscaled data might help us to know more about the first half of the century, where there is a lack of observations, and to improve our knowledge about the advantages and deficiencies of our decadal predictions over Europe. Finally, the here investigated RCSM can be used to



improve our knowledge about the future climate change in Europe, e.g. to simulate decadal predictions or climate projection ensembles, specially, in those areas close to the marginal seas. Examples of similar studies are Pham et al. (2018), where the added skill by coupling the Baltic and North Seas in decadal predictions is analysed, or Damarkis et al. (2019), where the future evolution of marine heatwaves in the Mediterranean Sea is studied.

## 5 Code and data availability

This paper describes an atmospheric-ocean coupled CCLM-NEMO system. The atmospheric CCLM model source code is freely available for scientific usage by members of the CLM-Community ([www.clm-community.eu](http://www.clm-community.eu)), a network of scientists who accept the CLM-Community agreement. To become a member, please contact the CLM-Community coordination office at DWD, Germany ([clm-coordination@dwd.de](mailto:clm-coordination@dwd.de)). The ice-ocean component set up for the North Sea and Baltic Sea (NEMO-Nordic) is released under the terms of the CeCill license (<http://www.cecill.info>, last access: 3 May 2019). It uses NEMO 3.3.1 with some changes and its code is available in the zenodo archive (<https://dx.doi.org/10.5281/zenodo.2643477>). The ocean component set up for the Mediterranean (NEMO-MED) uses NEMO 3.6. and its code is available under [https://prodn.idris.fr/thredds/fileServer/ipsl\\_public/rtron960/NEMO\\_MED\\_v3.6.tar](https://prodn.idris.fr/thredds/fileServer/ipsl_public/rtron960/NEMO_MED_v3.6.tar). The OASIS3-MCT coupling library can be downloaded at <https://verc.enes.org/oasis/>. Data presented in this work is also available for research purposes in the zenodo archive ([10.5281/zenodo.2659205](https://dx.doi.org/10.5281/zenodo.2659205)).

## Author contributions

C.P. performed the coupled simulation. H.F. performed the uncoupled simulation. C.P. and F.D.K. evaluated the simulations. B.A. conceived the experiment and contributed to the coupled system design. All authors discussed the results. C.P. took the lead in writing the manuscript with feedback and comments from all the authors.

## 20 Competing interests.

The authors declare that they have no conflict of interest.

## Acknowledgements

The authors acknowledge support by the German Research Foundation (“Deutsche Forschungsgemeinschaft”, DFG) in terms of the research group FOR 2416 “Space-Time Dynamics of Extreme Floods (SPATE)”, the German Federal Ministry of Education and Research (BMBF) under Grant MiKlip: FKZ01LP1518C/A and funding from the European Union’s Horizon 2020 research and innovation programme under grant agreement No 776661, entitled DownScaling CLimate ImPACTs and decarbonisation pathways in EU islands, and enhancing socioeconomic and non-market evaluation of Climate Change for Europe, for 2050 and Beyond. The opinions expressed are those of the author(s) only and should not be considered as representative of the European Commission’s official position.



The authors also thank the Centre for Scientific Computing (CSC) of the Goethe University Frankfurt and the German High-Performance Computing Centre for Climate and Earth System Research (“*Deutsches Klimarechenzentrum*”, DKRZ) for supporting the calculations.

Special thanks to Dr. Christian Dieterich and other colleagues from SMHI for providing the NEMO-NORDIC model and to  
5 Dr. Naveed Akhtar from HZG for helping with the coupled set-up.

## References

- Akhtar, N., Brauch, J. and Ahrens, B.: Climate modeling over the Mediterranean Sea: impact of resolution and ocean coupling, *Clim. Dyn.*, 51 (3), 933–948, doi:10.1007/s00382-017-3570-8, 2017.
- Balmaseda, M.A., Mogensen, K., and Weaver, A.T.: Evaluation of the ECMWF ocean reanalysis system ORAS4, *QJR Meteorol. Soc.*, 139, 1132–1161, doi: 10.1002/qj.2063, 2013.
- 10 Beuvier, J., Lebeaupin Brossier, C., Béranger, K., Arsouze, T., Bourdallé-Badie, R., Deltel, C., Drillet, Y., Drobinski, P., Ferry, N., Lyard, F., Sevault, F., and Somot, S.: MED12, Oceanic component for the modeling of the regional Mediterranean earth system, *Mercator Ocean Quarterly Newsletter*, 46, 2012.
- Casanueva, A., Rodríguez-Puebla, C., Frías, M. D., and González-Reviriego, N.: Variability of extreme precipitation over  
15 Europe and its relationships with teleconnection patterns, *Hydrol. Earth Syst. Sci.*, 18(2), 709–725, doi:10.5194/hess-18-709-2014, 2014.
- Christensen, J. H.: Prediction of Regional Scenarios and Uncertainties for Defining European Climate Change Risks and Effects (PRUDENCE), Final Report, DMI, 269p, 2005.
- Compo, G.P., J.S. Whitaker, P.D. Sardeshmukh, N. Matsui, R.J. Allan, X. Yin, B.E. Gleason, R.S. Vose, G. Rutledge, P.  
20 Bessemoulin, S. Brönnimann, M. Brunet, R.I. Crouthamel, A.N. Grant, P.Y. Groisman, P.D. Jones, M. Kruk, A.C. Kruger, G.J. Marshall, M. Maugeri, H.Y. Mok, Ø. Nordli, T.F. Ross, R.M. Trigo, X.L. Wang, S.D. Woodruff, and S.J. Worley: The Twentieth Century Reanalysis Project, *Quarterly J. Roy. Meteorol. Soc.*, 137, 1-28, doi: 10.1002/qj.776, 2011.
- Craig A., Valcke S., and Coquart L.: Development and performance of a new version of the OASIS coupler, *OASIS3-MCT\_3.0*, *Geoscientific Model Development*, 10, pp. 3297-3308, doi:10.5194/gmd-10-3297-2017, 2017.
- 25 Darmaraki, S., Somot, S., Sevault, F., Nabat, P., Cabos Narvaez, W. D., Cavicchia, L., Djurdjevic, V., Li, L., Sannino, G. and Sein, D.V.: Future Evolution of Marine Heatwaves in the Mediterranean Sea, *Clim. Dyn.*, 45, 1–22, doi:10.1007/s00382-019-04661-z, 2019.
- Dommenget, D.: Analysis of the model climate sensitivity spread forced by mean sea surface temperature biases, *J. Clim.* 25:7147–7162, 2012.
- 30 DWD Climate Data Center (CDC): Historical daily station observations (temperature, pressure, precipitation, sunshine duration, etc.) for Germany, version v005, 2017.



- Gasper, F., Goergen, K., Shrestha, P., Sulis, M., Rihani, J., Geimer, M., and Kollet, S.: Implementation and scaling of the fully coupled Terrestrial Systems Modeling Platform (TerrSysMP v1.0) in a massively parallel supercomputing environment – a case study on JUQUEEN (IBM Blue Gene/Q), *Geosci. Model Dev.*, 7, 2531–2543, doi:10.5194/gmd-7-2531-2014, 2014.
- Hartmann, D., Tank, A. K., Rusticucci, M., Alexander, L., Brönnimann, S., Charabi, Y., Dentener, F., Dlugokencky, E.,  
5 Easterling, D., Kaplan, A., Soden, B., Thorne, P., Wild, M., and Zhai, P.: Observations: atmosphere and surface - Climate Change 2013: the Physical Science Basis, EU-FP6 project ENSEMBLES & ECA&D project E-OBS gridded dataset, Website, accessed at 2016/1/22. <http://www.ecad.eu/download/ensembles/download.php>, 2016.
- Harris, I., Jones, P.D., Osborn, T.J., and Lister, D.H.: Updated high-resolution grids of monthly climatic observations – the CRU TS3.10 Dataset, *Int. J. Climatol.*, 34(3): 623–642, doi: 10.1002/joc.3711, 2014.
- 10 Haylock, M.R., Hofstra, N., Tank, A. K., Klok, E., Jones, P. and New, M.: A European daily high-resolution gridded dataset of surface temperature and precipitation, *J. Geophys. Res.*, 113, D20119, doi:10.1029/2008JD10201, 2008.
- Hordoir, R., Axell, L., Höglund, A., Dieterich, C., Fransner, F., Gröger, M., Liu, Y., Pemberton, P., Schimanke, S., Andersson, H., Ljungemyr, P., Nygren, P., Falahat, S., Nord, A., Jönsson, A., Lake, I., Döös, K., Hieronymus, M., Dietze, H., Löptien, U., Kuznetsov, I., Westerlund, A., Tuomi, L., and Haapala, J.: Nemo-Nordic 1.0: A NEMO based ocean model for Baltic & North  
15 Seas, research and operational applications, *Geoscientific Model Development Discussions*, 1–29, doi: 10.5194/gmd-2018-2, 2018.
- Jacob, R., Larson, J., and Ong, E.: M x N communication and parallel interpolation in Community Climate System Model Version 3 using the model coupling toolkit, *Int. J. High Perform. C.*, 19, 293–307, 2005.
- Jungclaus, J. H., Fischer, N., Haak, H., Lohmann, K., Marotzke, J., Matei, D., Mikolajewicz, U., Notz, D. and Storch, J. S.:  
20 Characteristics of the ocean simulations in MPIOM, the ocean component of the MPI-Earth system model, *J. Adv. Model. Earth Syst.*, 5, 422–446, 2013.
- Karl, T.R., Nicholls, N. and Ghazi, A.: CLIVAR/GCOS/WMO workshop on indices and indicators for climate extremes: Workshop summary. *Climatic Change*, 42, 3–7, 1999.
- Li, L., Bozec, A., Somot, S., Béranger, K., Bouruet-Aubertot, P., Sevault, F., and Crépon, M.: Regional atmospheric, marine  
25 processes and climate modelling, *Developments in Earth and Environmental Sciences*, Vol. 4, 373–397, doi:10.1016/s1571-9197(06)80010-8, 2006.
- Lindström, G., Pers, C.P., Rosberg, R., Strömqvist, J., and Arheimer, B.: Development and test of the HYPE (Hydrological Predictions for the Environment) model—A water quality model for different spatial scales. *Hydrol. Res.*, 41, 295–319, doi: 10.2166/nh.2010.007, 2010.
- 30 Ludwig, W., Dumont, E., Meybeck, M., and Heussner, S.: River discharges of water and nutrients to the Mediterranean and Black Sea: major drivers for ecosystem changes during past and future decades?, *Prog. Oceanogr.*, 80, 199–217, 2009.
- Maisonave, E. and Caubel, A.: LUCIA, load balancing tool for OASIS coupled systems, TR-CMGC 14-63, CERFACS, 2014.
- Madec, G.: NEMO ocean engine (version 3.3), Tech. Rep. 27, Note du Pole de modélisation, Institut Pierre- Simon Laplace (IPSL), France, 2011.





- Marotzke, J., W.A. Müller, F.S. Vamborg, P. Becker, U. Cubasch, H. Feldmann, F. Kaspar, C. Kottmeier, C. Marini, I. Polkova, K. Prömmel, H.W. Rust, D. Stammer, U. Ulbrich, C. Kadow, A. Köhl, J. Kröger, T. Kruschke, J.G. Pinto, H. Pohlmann, M. Reyers, M. Schröder, F. Sienz, C. Timmreck, and M. Ziese: [MiKlip: A National Research Project on Decadal Climate Prediction](#). *Bull. Amer. Meteor. Soc.*, 97, 2379–2394, doi:10.1175/BAMS-D-15-00184.1, 2016.
- 5 Müller, W.A., Matei, D., Bersch, M., Jungclaus, J.H., Haak, H., Lohmann, K., Compo, P., Sardeshmukh, D., and Marotzke, J.: A twentieth-century reanalysis forced ocean model to reconstruct the North Atlantic climate variations during the 1920s., *Clim Dyn* 44:1935–1955, doi:10.1007/s00382-014-2267-5, 2015.
- Müller, W. A., Pohlmann, H., Sienz, F., Smith, D.: Decadal climate prediction for the period 1901-2010 with a coupled climate model. *Geophys. Res. Lett.*, 41, pp 2100-2107, doi:10.1002/2014GL059259, 2014.
- 10 Obermann, A., Bastin, S., Belamari, S. Conte, D., Gaertner, M.A., Li, L. and Ahrens, B.: Mistral and Tramontane wind speed and wind direction patterns in regional climate simulations, *Clim. Dyn.*, 51(3), 1059-1076, doi:10.1007/s00382-016-3053-3, 2018.
- Pham, T., Brauch, J., Dieterich, D., Früh, B., and Ahrens, B.: New coupled atmosphere-ocean-ice system COSMO-CLM/NEMO: On the air temperature sensitivity on the North and Baltic Seas, *Oceanologia*, 56, 167–189, doi:10.5697/oc.56-2.167, 2014.
- 15 Pham, T., Brauch, J., Dieterich, D., Früh, B., and Ahrens, B.: Added Decadal Prediction Skill with the Coupled Regional Climate Model COSMO-CLM/NEMO, *Meteorologische Zeitschrift* 27 (5), 391–99, doi:10.1127/metz/2018/0872, 2018.
- Rayner, N. A., Parker, D. E., Horton, E. B., Folland, C. K., Alexander L. V., Rowell, D. P., Kent, E.C. and Kaplan, A.: Global analyses of sea surface temperature, sea ice, and night marine air temperature since the late nineteenth century, *J. Geophys. Res.*, Vol. 108, No. D14, 4407, doi:10.1029/2002JD002670, 2003.
- Reynolds, R. W., Rayner, N. A., Smith, T. M., Stokes, D. C. and Wang, W.: An improved in situ and satellite SST analysis for climate. *J. Clim.* 15, 1609–1625, 2002.
- Rixen, M.: MEDAR/MEDATLAS-II, GAME/CNRM, doi:10.6096/HyMeX.MEDAR/MEDATLAS-II.20120112, 2012.
- Rockel, B., Will, A., and Hense, A.: The Regional Climate Model CLM, *Meteorol. Z.*, 17, 347–348, 2008.
- 25 Rummukainen, M., Ræisaenen, J., Bringfelt, B., Ullerstig, A., Omstedt, A., Willen, U., Hansson, U., and Jones, C.: A regional climate model for northern Europe: model description and results from the downscaling of two GCM control simulations, *Clim. Dyn.*, 17, 339–359, 2001.
- Schrum, C.: Thermohaline stratification and instabilities at tidal mixing fronts. Results of an eddy resolving model for the German Bight, *Continental Shelf Research*, 17,(6), 689-716, 1997.
- 30 Schrum, C., U. Hubner, D. Jacob, and R. Podzun.: A Coupled Atmosphere-Ice-Ocean Model for the North Sea and the Baltic Sea, *Climate Dynamica*, 21: 123–145, 2003.
- Sevault, F., Somot, S., Alias, A., Dubois, C., Lebeaupin- Brossier, C., Nabat, P., Adloff, F., Déqué, M., and Decharme, B.: A fully coupled Mediterranean regional climate system model: design and evaluation of the ocean component for the 1980–2012 period, *Tellus A*, 66, 23967, doi:10.3402/tellusa.v66.23967, 2014.



- Somot, S., Sevault, F., Déqué, M., and Crépon, M.: 21st century climate change scenario for the Mediterranean using a coupled Atmosphere-Ocean Regional Climate Model, *Global and Planetary Change*, 63, 112–126, doi:10.1016/j.gloplacha.2007.10.003, 2008.
- Stevens, B., Giorgetta, M., Esch, M., Mauritsen, T., Crueger, T., Rast, S., Salzmann, M., Schmidt, H., Bader, J., Block, K.,  
5 Brokopf, R., Fast, I., Kinne, S., Kornbluh, L., Lohmann, U., Pincus, R., Reichler, T. and Roeckner, E.: Atmospheric component of the MPI-M Earth System Model: ECHAM6, *J. Adv. Model. Earth Syst.*, 5, 1590–1601, doi:10.1002/jame.20015, 2013.
- Sun, Y., Solomon, S., Dai, A., and Portmann, R.W.: How often does it rain?, *J. Clim.*, 19, 916–934, doi: 10.1175/JCLI3672.1, 2006.
- 10 Tebaldi, C., Hayhoe, K., Arblaster, J. M., and Meehl, G. A.: Going to the extremes: an intercomparison of model simulated historical and future changes in extreme events, *Climatic Change*, 3–4, 185–211, 2006.
- University of East Anglia Climatic Research Unit; Harris, I.C.; Jones, P.D.: CRU TS4.01: Climatic Research Unit (CRU) Time-Series (TS) version 4.01 of high-resolution gridded data of month-by-month variation in climate (Jan. 1901- Dec. 2016). Centre for Environmental Data Analysis, 04 December 2017. doi:10.5285/58a8802721c94c66ae45c3baa4d814d0, 2017.
- 15 Vancoppenolle, M., Fichefet, T., Goosse, H., Bouillon, S., Madec, G. and Morales Maqueda, M.A.: Simulating the mass balance and salinity of Arctic and Antarctic sea ice. 1. Model description and validation. *Ocean Modelling*, 27, 33-53, doi:10.1016/j.oceanmod.2008.10.005, 2009.
- Will, A., Akhtar, N., Brauch, J., Breil, M., Davin, E., Ho-Hagemann, H., Maisonnaive, E., Thürkow, M. and Weiher, S.: The regional climate model and the model components coupled via OASIS-MCT: description and performance. *Geoscientific Model Development*, Vol. 10 (4), pp. 1549–1586, 2017.
- Zhang, X. B., G. Hegerl, F. W. Zwiers, and J. Kenyon: Avoiding inhomogeneity in percentile-based indices of temperature extremes, *J. Climate*, 18, 1641, 2005.
- Zhang, X., Alexander, L., Hegerl, G. C., Jones, P., Tank, A.K., Peterson, T.C., Trewin, B., Zwiers, F.W.: Indices for monitoring changes in extremes based on daily temperature and precipitation data. *WIREs Clim Change*, 2: 851-870.  
25 doi:10.1002/wcc.147, 2011.



## Figures

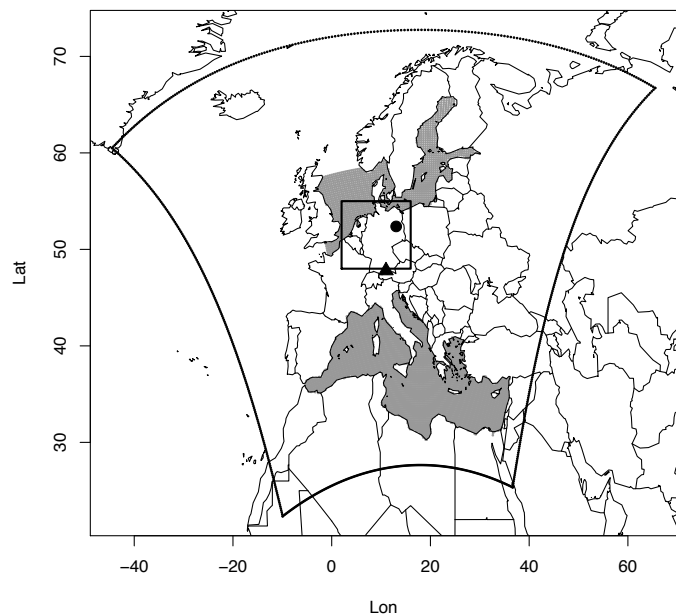


Figure 1: EURO-CORDEX domain where the coupled system runs, including the marginal seas (grey area), the Mid-Europe region from the PRUDENCE project (square) and two locations of German climate stations: Potsdam (circle) and Hohenpeißenberg (triangle).

5

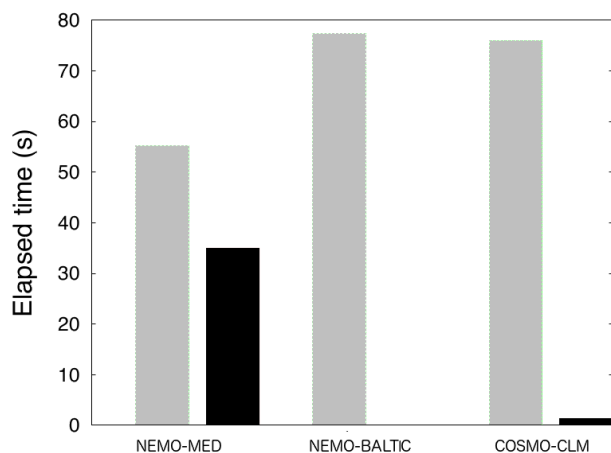
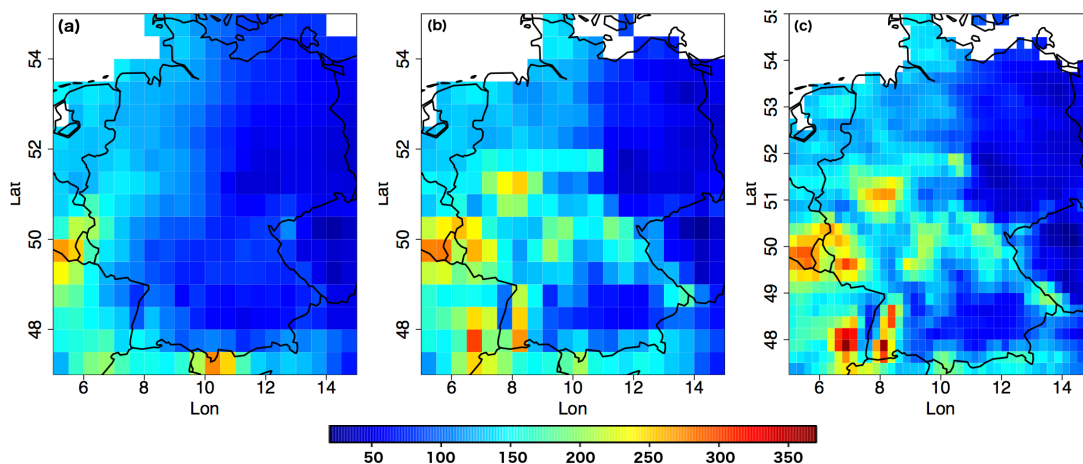
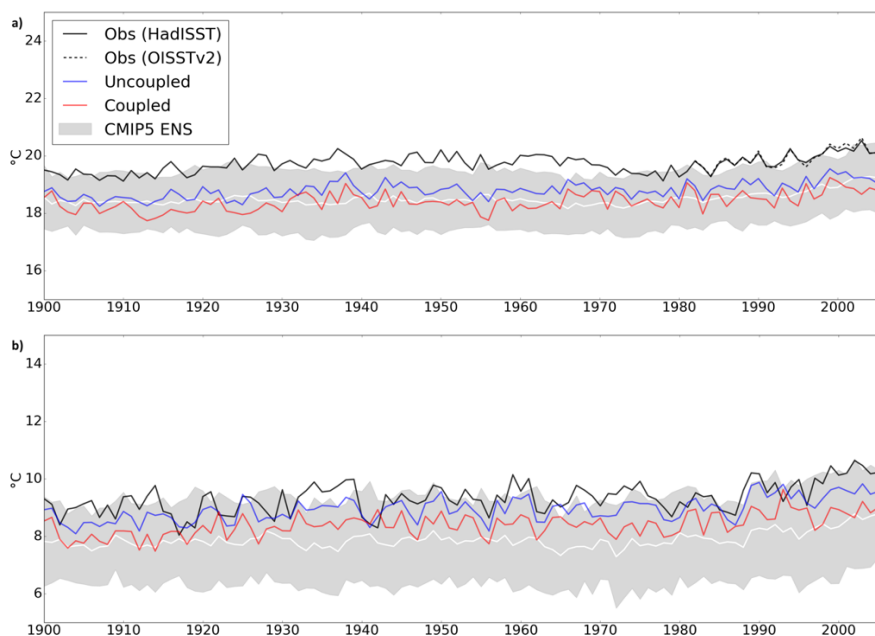


Figure 2: Computing time used for the exchange of each of the OASIS coupled model components. Grey bars show calculation time and black bars show waiting time.



5 **Figure 3:** Total precipitation observations in January 1995: (a) CRU data ( $0.5^\circ \times 0.5^\circ$ ), (b) upscaled to  $0.5^\circ \times 0.5^\circ$  version of the EObs data and (c) the original EObs resolution ( $0.25^\circ \times 0.25^\circ$ ).



10 **Figure 4:** Sea surface temperature annual means over the marginal seas in our 20<sup>th</sup> Century coupled simulation (CCLM-NEMO) between 1900 and 2005, compared to observations (HadISST and in case of the Mediterranean also OISSTv2), to the atmosphere-only CCLM simulation (with prescribed SST by the driving MPI-ESM-LR as20NCEP simulation), and an ensemble mean (white line) and spread (shaded area) from CMIP5 simulations. a) Mediterranean Sea and b) Baltic and North Sea.

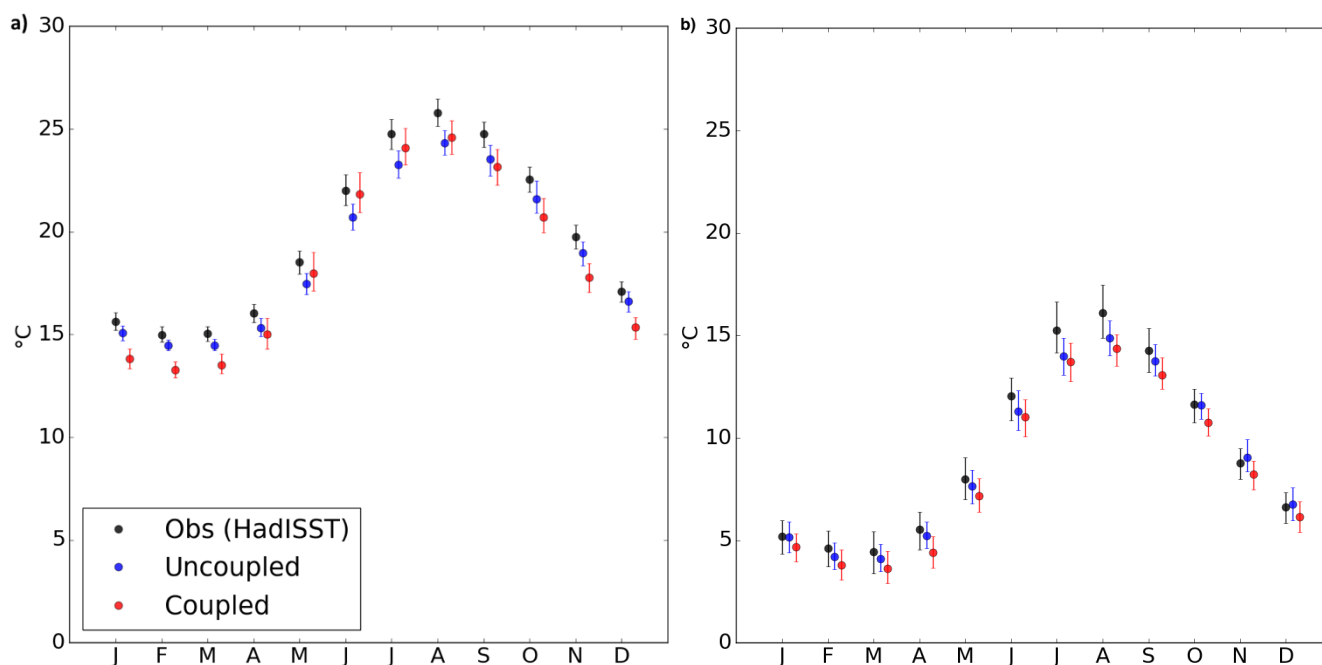
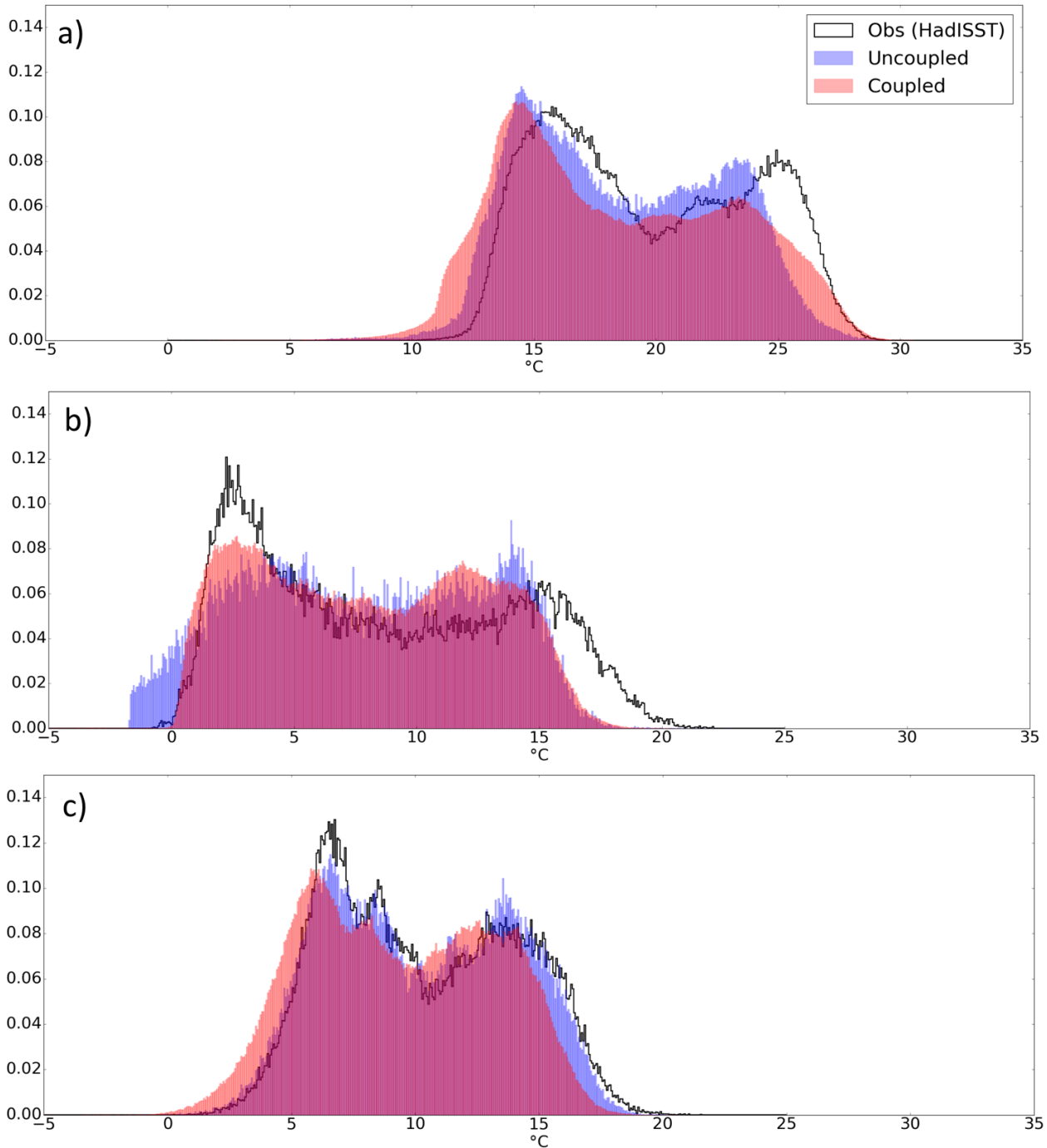
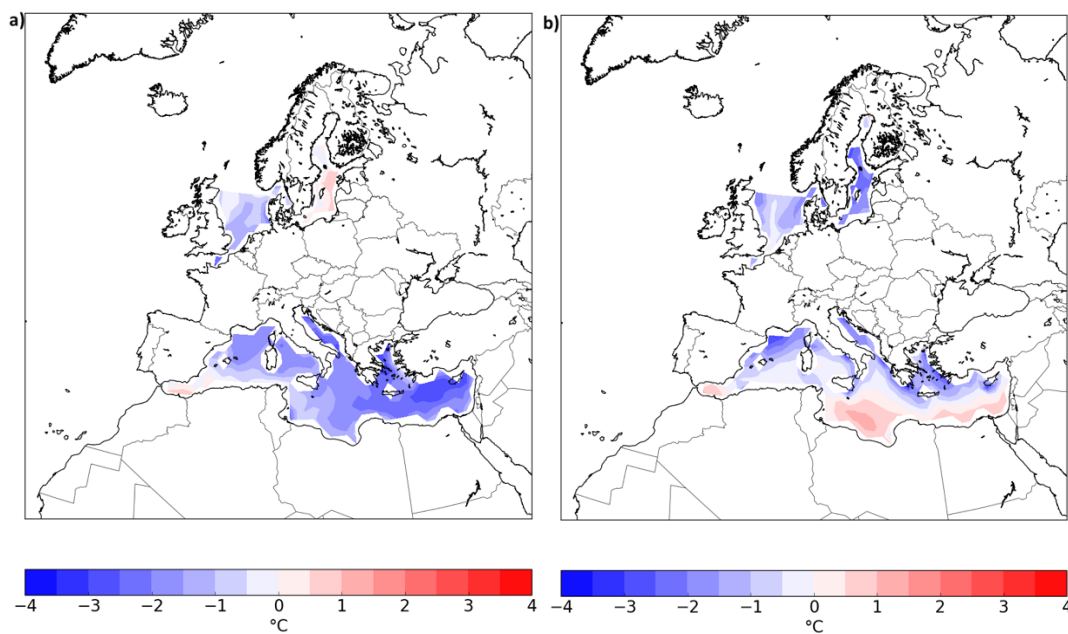


Figure 5: Annual cycle spatial mean SST values in the marginal seas a) Mediterranean Sea b) Baltic and North Sea. Dots represent the monthly averaged value and intervals show the 10<sup>th</sup> and 90<sup>th</sup> percentiles.

5



**Figure 6: Density histograms of SST values in the marginal seas a) Mediterranean Sea b) Baltic Sea and c) North Sea. Note that in case of the Baltic Sea the grid points containing sea ice are filtered out.**



**Figure 7:** a) Winter and b) summer SST spatial distribution difference between the coupled simulation and the observation.

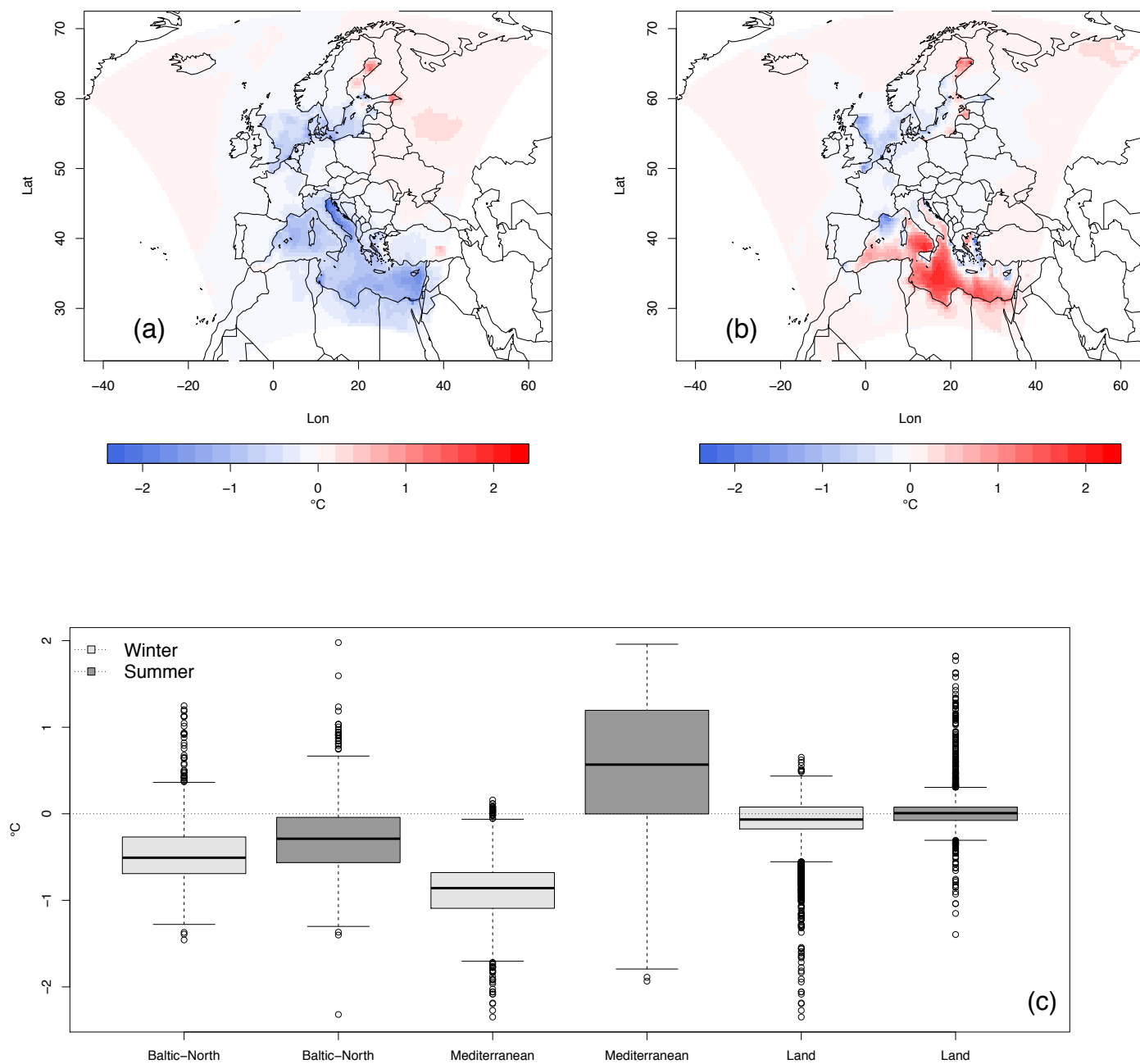


**Figure 8: Differences between the coupled and uncoupled simulations of the 2m-temperature monthly mean (°C) averaged over the 20<sup>th</sup> century during winter (a) and summer (b). Boxplots represent the distributions of the monthly mean over the marginal seas and land separately (c).**



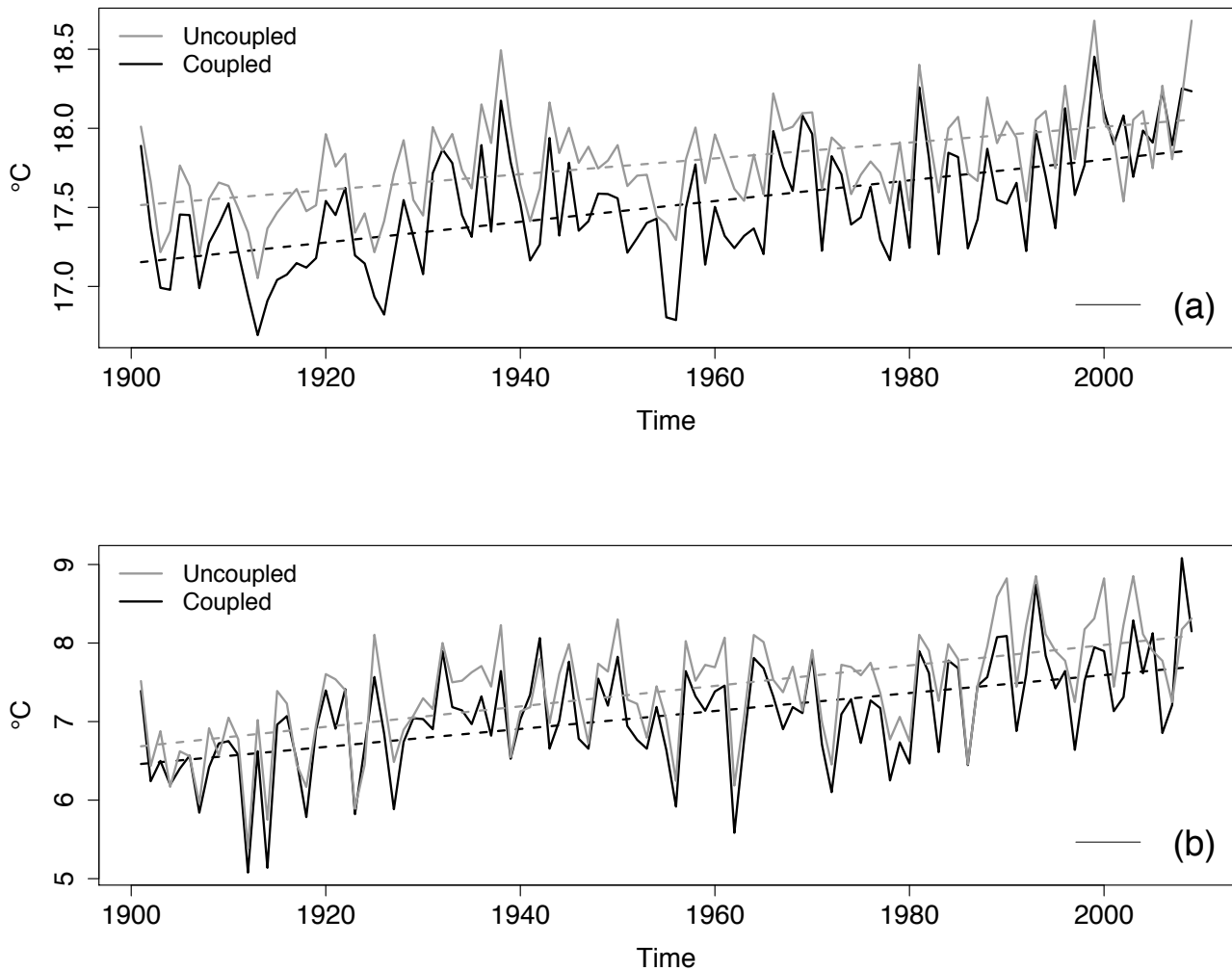


**Figure 9: Temporal evolution of the 2m-temperature annual mean averaged over the Mediterranean Sea (a) and the Baltic and North Seas (b). Dashed lines represent a linear fit.**

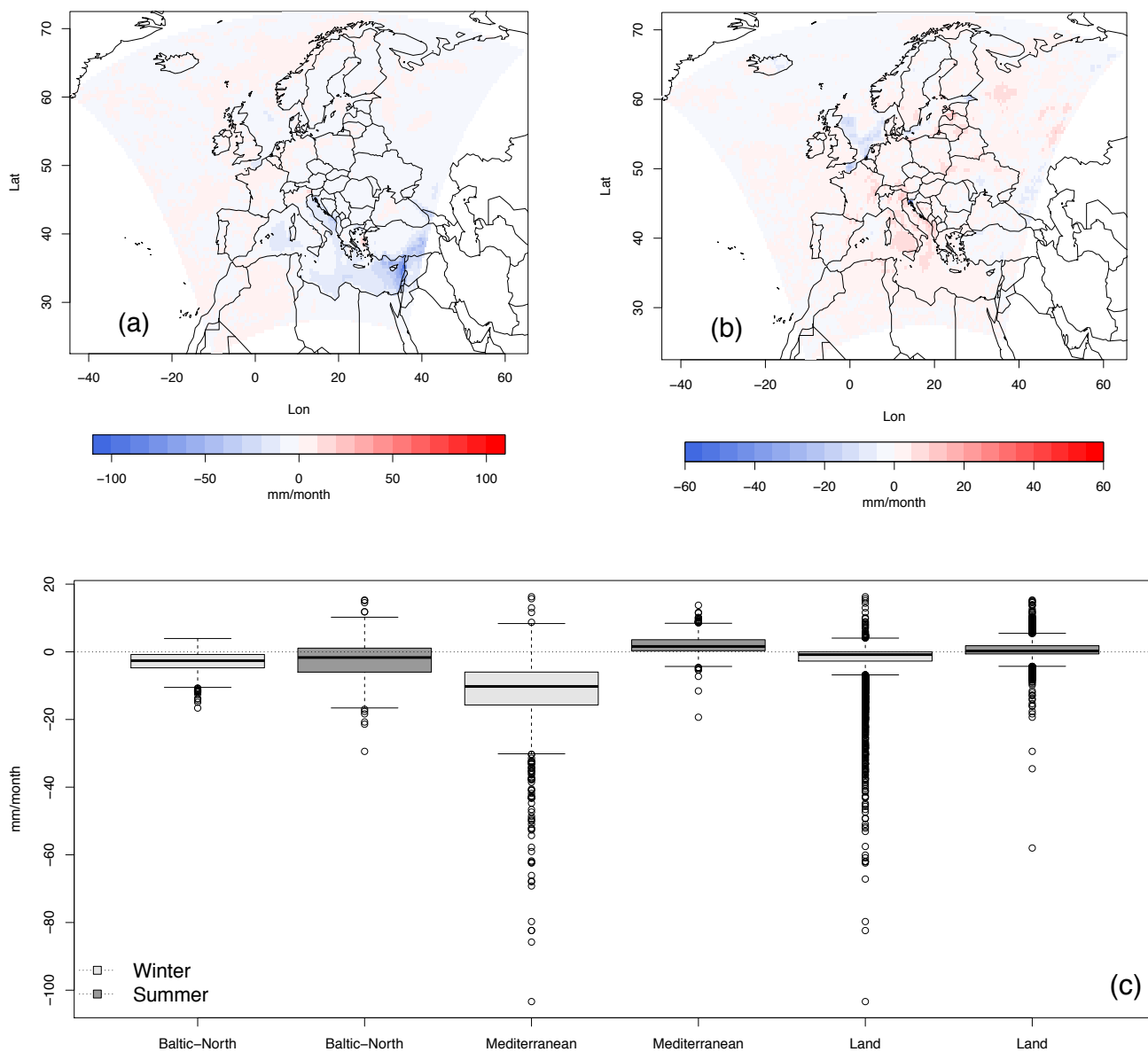
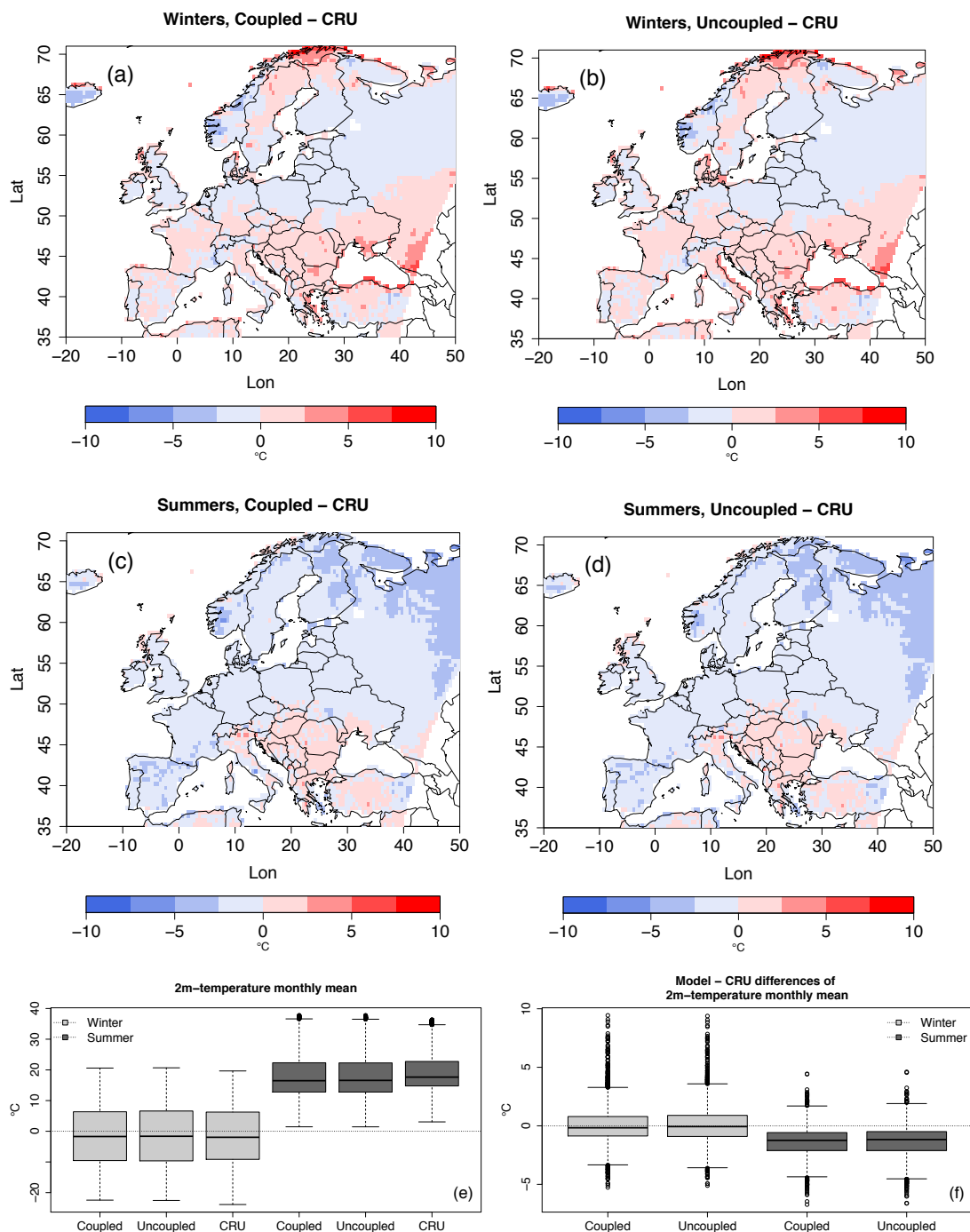


**Figure 10: Differences between the total precipitation monthly sum of the coupled and uncoupled systems, averaged over winter (a) and summer (b) for the period 1901-2009. Boxplots (c) represent the distribution of these differences over the marginal seas and land separately.**



5 **Figure 11: 2m-Temperature differences between the coupled system and CRU data (a, c) and the uncoupled system and CRU data (b, d), during winter (a, b) and summer (c, d) for the 20<sup>th</sup> century. Boxplots of the 2m-temperature (e) and boxplots of the differences between regional models and CRU (f).**

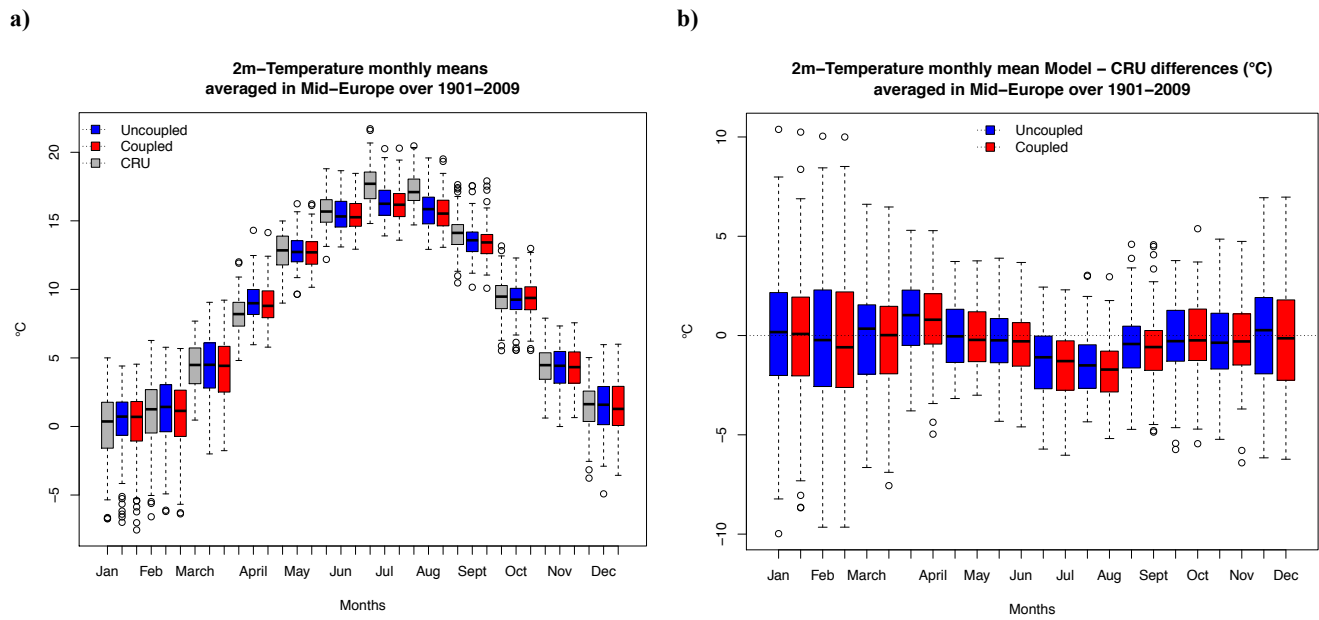


**Figure 12: Boxplots showing the annual cycle during the 20<sup>th</sup> century of the 2m-Temperature monthly means averaged over Mid-Europe for the CRU observations (grey), uncoupled system (blue) and coupled system (red) (a) and the annual cycle of the model errors compared to CRU observations over Mid-Europe (b).**

5

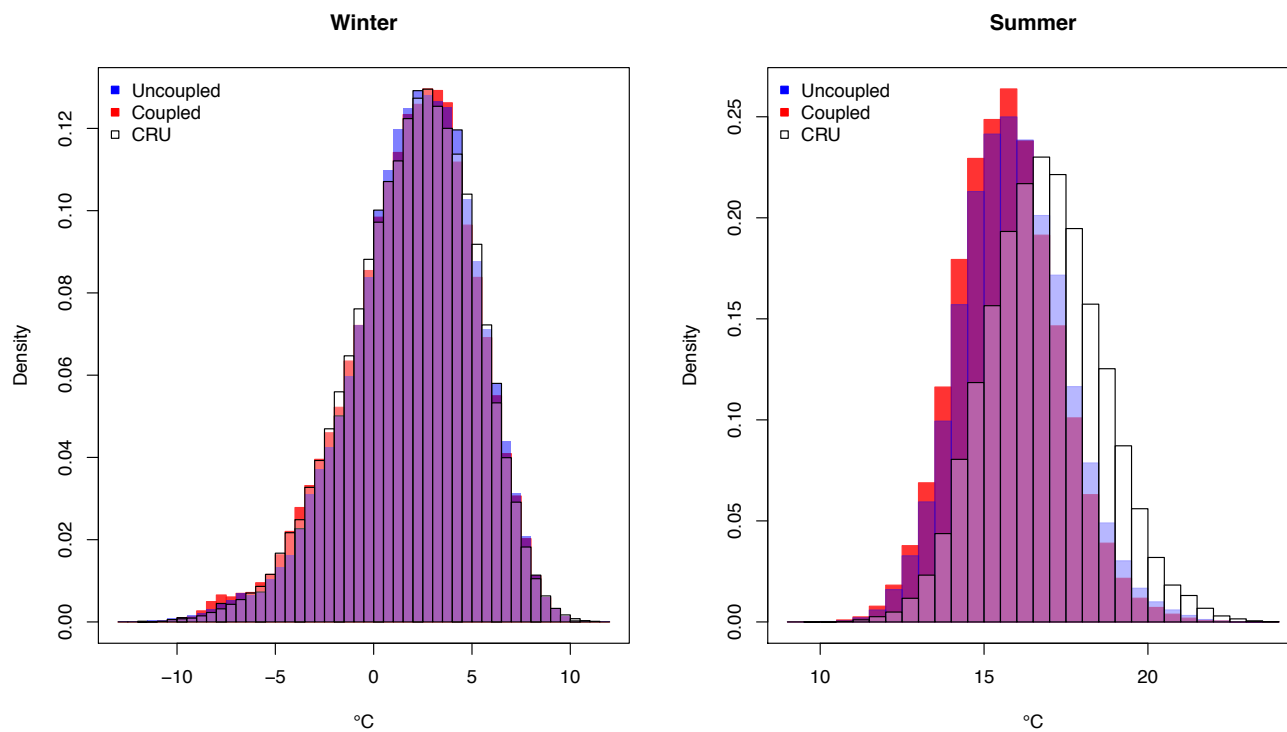
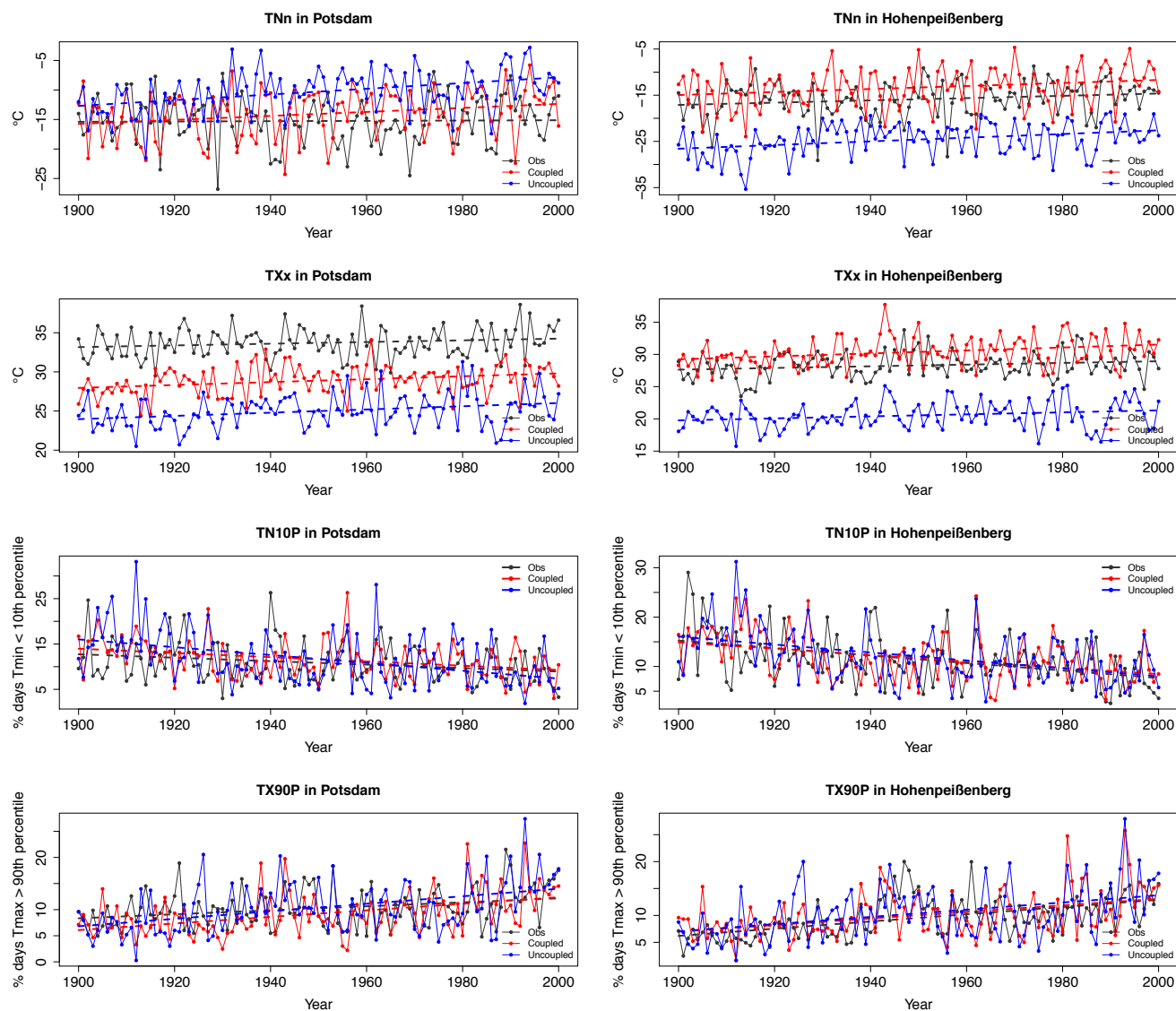


**Figure 13: 2m-Temperature histograms of the coupled and uncoupled systems compared to the CRU data over the PRUDENCE area named Mid-Europe during the 20<sup>th</sup> century in winter (left) and summer (right).**



5 **Figure 14: Temporal evolution of four climate change indices in two stations of Germany, Potsdam (81m) and Hohenpeißenberg (977m). TNn represents the annual minimum value of daily minimum temperature; TXx, the annual maximum value of daily maximum temperature; TX90p, the percentage of days when the maximum temperature is above the calendar day 90<sup>th</sup> percentile centred on a 5-day window for the base period 1961-1990. TN10p, the percentage of days when the minimum temperature is below the calendar day 10<sup>th</sup> percentile centred on a 5-day window for the base period 1961-1990. Linear trends are shown as dashed lines.**

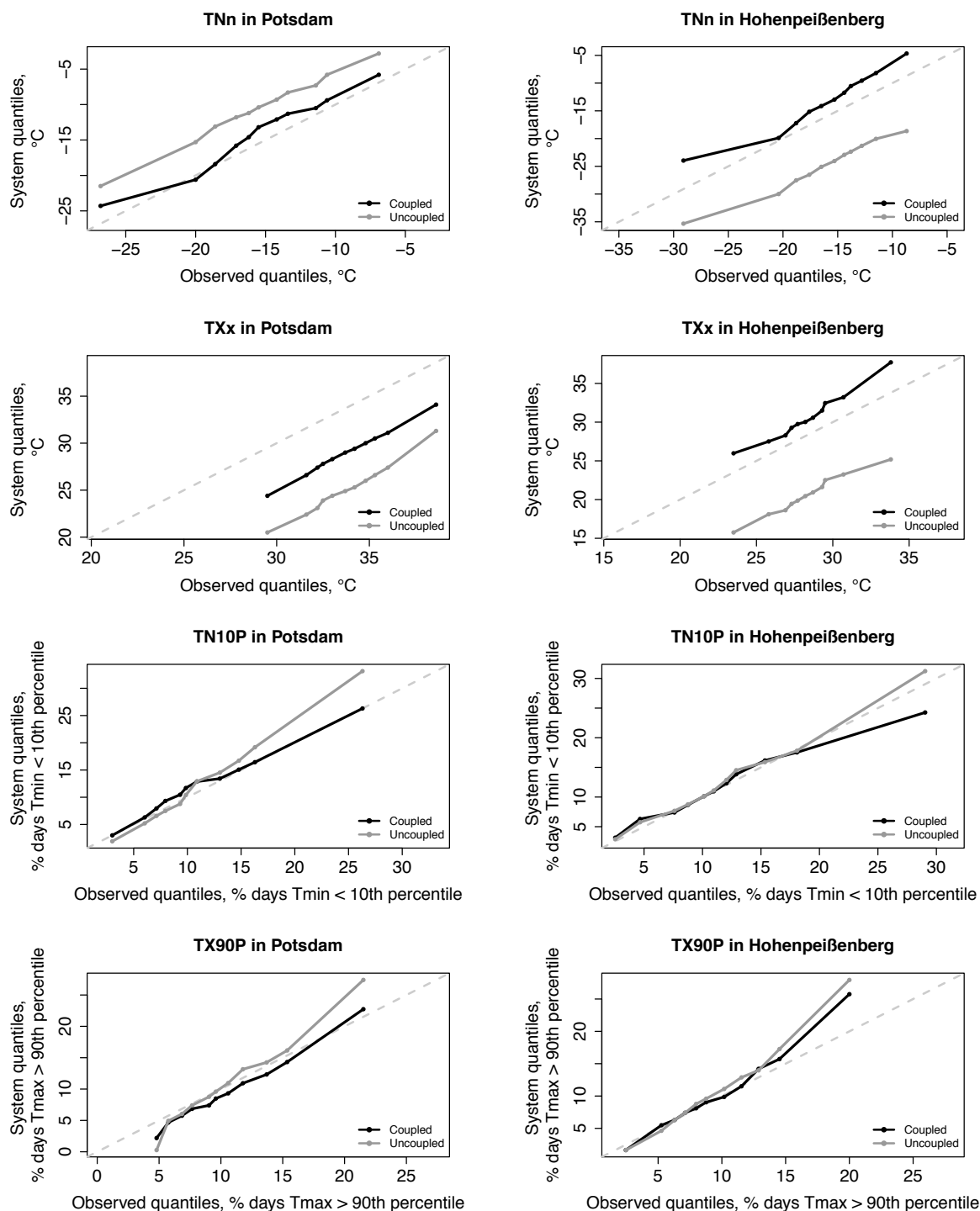
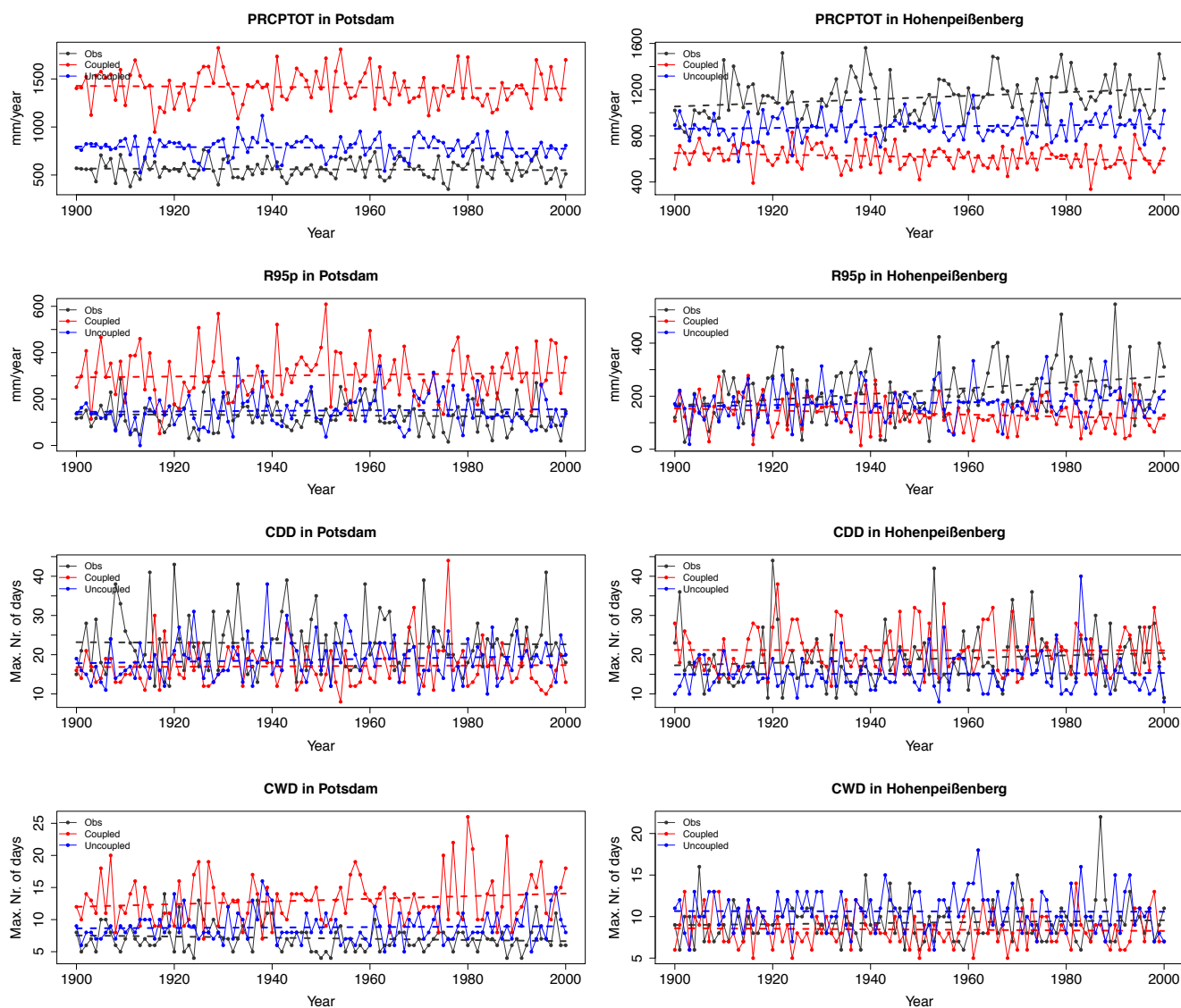


**Figure 15:** q-q plot of the extreme indices represented in Fig.14 for the CRU observed data and the coupled (black lines) and the uncoupled (grey lines) systems. The diagonal represents the perfect case.



5 **Figure 16: Temporal evolution of four climate change indices related to precipitation in two German stations: Potsdam (81m) and Hohenpeißenberg (977m). PRCPTOT represents the annual total precipitation in wet days, R95p is the annual total PRCP when the daily precipitation (RR) is above the 95<sup>th</sup> percentile of precipitation on wet days in the 1961-1990 period, CDD is the maximum length of dry spell (maximum number of consecutive days with RR < 1mm) and CWD is the maximum length of wet spell (maximum number of consecutive days with RR ≥ 1mm). Linear trends are shown as dashed lines.**



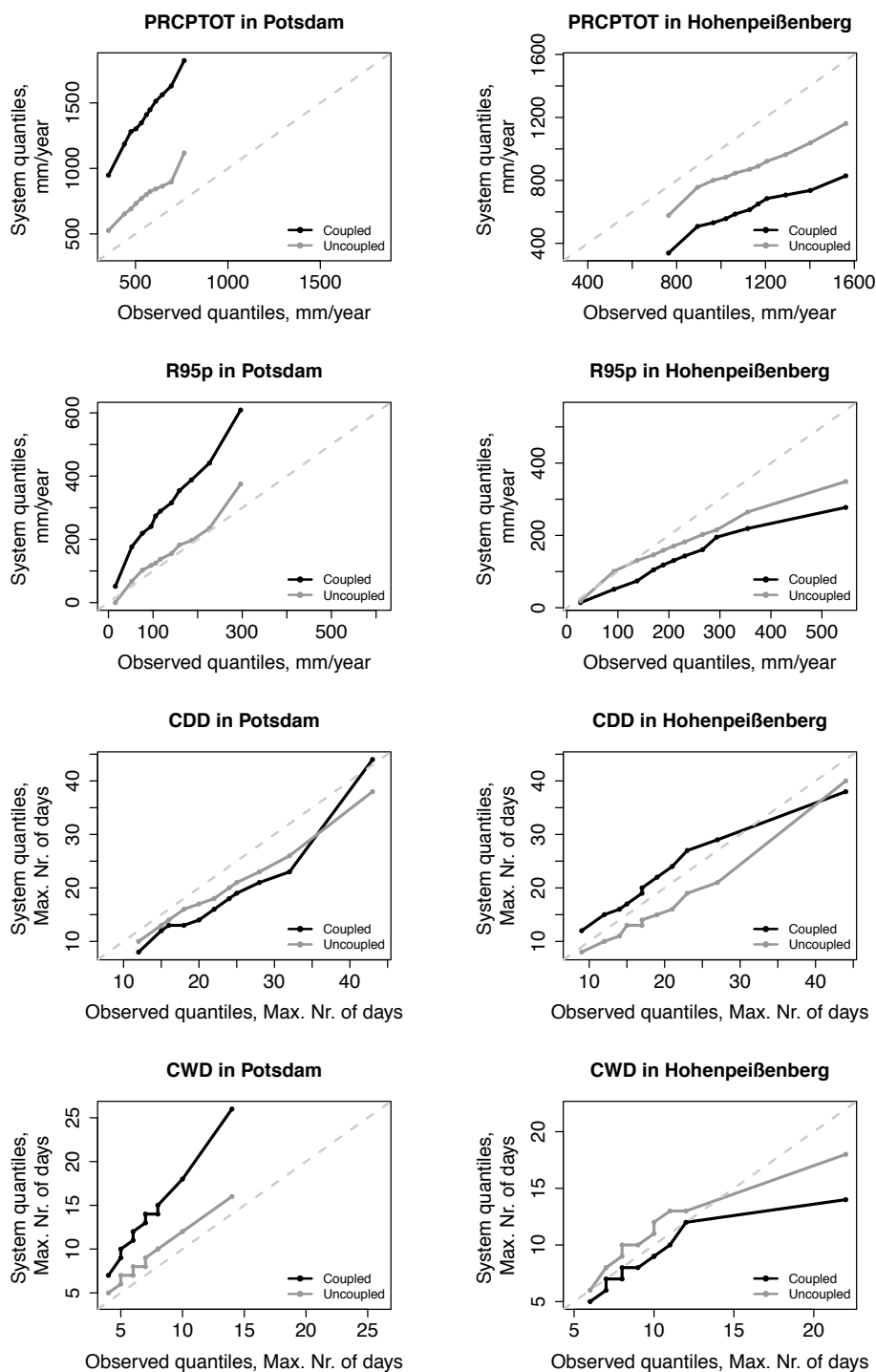


**Figure 17:** q-q plot of the extreme indices represented in Figure 16 for the CRU observed data and the coupled (black lines) and the uncoupled (grey lines) systems. The diagonal represents the perfect case.